

# Fenestration integrated BIPV (FIPV): A Review

Aritra Ghosh<sup>1</sup>

<sup>1</sup>College of Engineering, Mathematics and Physical Sciences, Renewable Energy, University of Exeter, Cornwall, TR10 9FE, UK

\*Corresponding author: [a.ghosh@exeter.ac.uk](mailto:a.ghosh@exeter.ac.uk)

## Abstract:

Building fenestrations are the key components maintaining the connection between building exterior and interior. However, they are also the weakest allowing heat loss, gain and light. To tackle the enhanced building energy demand, active and passive both ways must be included. Benign energy-generating components and passive energy-saving are both concomitantly possible using photovoltaic (PV) window fenestration. In this work, three different generations PV based fenestration integrated photovoltaics (FIPV) have been reviewed to understand how effective FIPVs are for low energy building. Later advanced technologies suitable for FIPV applications are also discussed.

**Keywords:** FIPV, BIPV, windows, CCT, CRI, *U*-value, SHGC, CdTe, a-Si, CIGS, DSSC, Perovskite, Organic, Switchable BIPV

## 1. Introduction

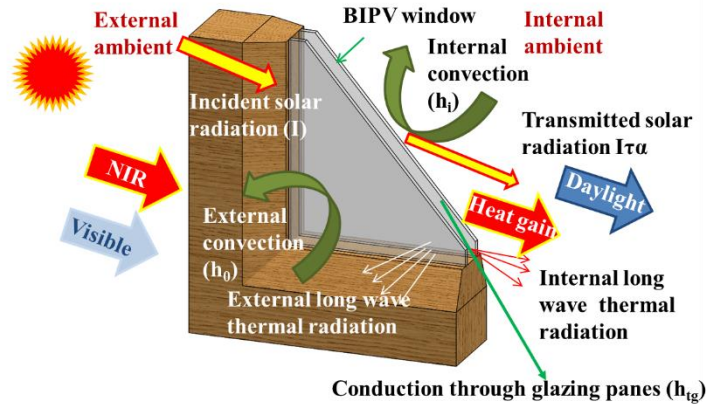
The building is one of the places where humans spend 90% of their time. Hence building interior health hugely influence the mood, wellbeing, and cognitive work producibility of buildings occupant. Depending on the local climate building needs heating, cooling, and lighting energy to create a soothing comfortable indoor environment (Nundy et al., 2021b). This excessive energy is required because of the diurnal variation of the external ambient. Low thermally insulated building envelope such as window, wall, and roof allows external heat to penetrate inside the building or internal heat to outside. In a hot climate dominated modern cities, buildings are fully air-conditioned which consume a considerable amount of fossil fuel-generated energy (Feng et al., 2021). In a cold climate, buildings require a heating load. Glazed units are an essential part of buildings' envelopes which provides views from interior to exterior, allow natural light and solar heat into a building's interior space. Compared to other building envelopes, the thermal performance of glazed windows is poorer. About 50% of the total energy consumption within buildings occurs through heat loss or gain via their windows, which increased significantly over the last decades (Nundy and Ghosh, 2020). From a sustainable point of view, a building should have protection from unwanted light, heat, air flow and low or zero consumption of energy. A window has a considerable amount of impact on the buildings lighting, heating and ventilation, hence overall building energy performance is influenced by the window. Building windows are also responsible for the building interior health and wellbeing. In the USA, window accounts for 25% of the utility bill of a household (Feng et al., 2020). Also, now there is a high demand for glazed facades based building architecture specially commercial building.

### 1.1. Overview of FIPV (BIPV window)

Hence, traditional building windows or fenestrations need to be replaced with an advanced system that has the potential to work with better capacity. Photovoltaic (PV) window is currently a major investigating area. PV system which generates benign energy in the presence of solar radiation can be employed in a building in the form of a window (Skandalos and Karamanis, 2015). As PV window is a part of a building, they can also be termed building integrated photovoltaic (BIPV) window. In general, the integration of PV systems in the building by replacing traditional building envelopes such as a wall,

45 roof, and window is termed BIPV (Kabilan et al., 2021; Kaliappan et al., 2021; Karthick et al., 2018b;  
46 Kumar et al., 2021; Singh et al., 2021). According to IEA Task 15, PV modules are only considered to  
47 be building integrated if it provides “(i) mechanical rigidity or structural integrity (ii) primary weather  
48 impact protection: rain, snow, wind, hail, (iii) energy economy such as shading, daylighting or thermal  
49 insulation, (iv) fire protection, (v) noise protection” (Iea-pvps, 2018). Integration of PV devices into a  
50 building is now growing rapidly (Ghosh, 2020a). Due to the inadequate space in urban regions, a cogent  
51 choice for PV technology applications is to integrate them into buildings (Chandrika et al., 2021;  
52 Karthick et al., 2020). These building integrated photovoltaic (BIPV) trim down the construction and  
53 material cost and electricity cost of a building. Transparent or semi-transparency is the precondition for  
54 the BIPV window (Ghosh, 2020a). For BIPV applications, electricity generation from PV is not only  
55 the main focus. Overall building energy performance in terms of heating, cooling and daylighting are  
56 also considered. However, currently opaque PV based BIPV is also considered such as BIPV tiles  
57 (Ballif et al., 2018; Kuhn et al., 2021). Also coloured PV cells are often employed to hide the PV  
58 functionalities and aesthetic application(Ghosh, 2020a).

59 Fenestration integrated PV (FIPV) or BIPV window is gaining prime importance as traditional single  
60 or double panes fenestration technologies are not energy efficient. To obtain maximum potential from  
61 FIPV, transparency, orientation (azimuth, tilt angle, and building self-shading), PV devices  
62 temperature, window-to-wall ratio, coverage, fresh air infiltration, the mass of the floor and ceiling,  
63 solar heat gain coefficient, conversion efficiency, should be considered according to the surrounding  
64 climatic conditions. The primary purpose of a window is to allow visual and thermal comfort into an  
65 interior of a building. Thus, to understand the potential to attain thermal and visual comfort from the  
66 BIPV window, understanding these parameters are essential. **Figure 1** represents heat and light transfer  
67 mechanisms of a BIPV window (excluding power generation). BIPV window’s visual comfort includes  
68 comfortable daylight (Knoop et al., 2020; Quek et al., 2021), glare (Wienold et al., 2019; Wienold and  
69 Christoffersen, 2006), correlated color temperature (CCT) and color rendering index (CRI) (Ghosh and  
70 Norton, 2017a). External daylight penetrated through the BIPV window and reach to building interior  
71 should be between 100-2000 lux (Nabil and Mardaljevic, 2006). Above this range is identified as  
72 discomfort due to glare. Glare analysis can be done by using DGP or DGI methods. Transmitted  
73 daylight through the BIPV window experiences spectrum changes which may create issues for  
74 occupants. Understanding these CCT and CRI studies is worthwhile. The most desirable criteria are  
75 CRI which should be over 80 (out of 100) and CCT between 3000-7500 K. To realize the thermal  
76 comfort the key factors are overall heat transfer coefficient or thermal energy transmission ( $U$ -value)  
77 and solar heat gain coefficient or solar energy transmission or solar factor (SHGC/SF).  $U$ -value (in  
78  $W/m^2K$ ) is a heat-insulating property of glazing which includes heat loss from an outer surface of FIPV  
79 to ambient, heat loss from an interior surface to an internal ambient and heat loss from the thermal  
80 conduction through the glass panes. For a typical single- and double-glazing air-filled window,  $U$ -  
81 values are 3-5  $W/m^2K$  and 2-2.99  $W/m^2K$  respectively. Some providers are able to offer double glazing  
82 having  $U$ -value of 1.9 (Pilkington glass).  $U$ -value can further be reduced by increasing the glass  
83 thickness or number of glasses (Cerne et al., 2019), filled the air gap with inert gas, aerogel (Buratti et  
84 al., 2021) or make it vacuum (Ghosh et al., 2017, 2016a). SHGC indicates the fraction of transmitted  
85 solar radiation through the glazing and this unit less number varies between 0.1 to 1. A glazing having  
86 0.5 SHGC indicates that 50% solar radiation admitted through the glazing (Tait, 2006).  $U$ -value and  
87 SHGC also deal with building interior room comfortable temperature ( $\sim 18-20^{\circ}C$ ) which eventually  
88 predicts the thermal comfort. High SHGC of glazing is beneficial for cold climatic areas and hot climate  
89 it increases the cooling load demand of building. High  $U$ -value of glazing is beneficial for the hot  
90 climate while in winter it increases the heating load of a building. Estimation of buildings windows  
91 overall performance is essential as they have may have an impact from humidity, UV from the sun.  
92 This is more prominent in the case of BIPV type windows where PV material may be sensitive to  
93 external weather.



94

95 Figure 1: Schematic of BIPV window (FIPV) showing different heat transfer mechanisms.

96 In this work, a detailed review based on fenestration integrated PV (FIPV) or BIPV window has been  
 97 reviewed. BIPV window-based review is very rare. This work critically reviewed three-generation PV  
 98 cells for FIPV application and other advanced technologies. The structure of this work is as follows:  
 99 section 2 discussed the methodology applied to perform this review work, section 3 illustrated the first  
 100 generation, second generation and third generation PV based FIPV, section 4 introduced advanced  
 101 BIPV window, Section 5 discussion and perspective while section 6 concluded the overall work.

102

## 103 2. Methodology

104

105 Currently, advanced fenestration technologies are gaining importance because of their building energy-  
 106 saving property (Gorgolis and Karamanis, 2016; Rezaei et al., 2017). Fenestration or window  
 107 technologies generally possess static transparency. Single and double glazing windows which  
 108 dominated the building window industry for years after years now should be replaced. Currently, the  
 109 windows industry possess static and dynamic transparent window (Ghosh and Norton, 2018). Most  
 110 often static transparent advanced windows are capable to control the heat loss from the building interior  
 111 to the Exterior e.g. evacuated, aerogel glazing, low-e coated and inert gas-filled. On the other hand,  
 112 dynamic windows control SHGC and daylight e.g. phase change material, thermochromic (Tällberg et  
 113 al., 2019), thermotropic (Aburas et al., 2019), gasochromic (Feng et al., 2016), electrochromic,  
 114 suspended particle (Ghosh and Norton, 2019) and polymer dispersed liquid crystal (PDLC)(Ghosh et  
 115 al., 2018a) types. Among them, BIPV windows are different as they not only control the SHGC and  
 116 daylight but also generates benign electricity. Advanced windows are considered energy-saving  
 117 elements which employ a passive way. However, advanced BIPV windows work in both active and  
 118 passive ways and they can be built in such a way that can be influential for both hot and cold climates  
 119 both. This review is limited to the only BIPV window and its derivatives. There are many different  
 120 directions are available in the research area with BIPV system such as BIPVT, investigation of new  
 121 material for BIPV window or FIPV, PV shading element. In this work, we strictly concentrated on the  
 122 BIPV window. Other elements were not considered as from aesthetic point of view those are still not  
 123 mature. Also, we focused on those elements which at least reached high technological readiness level.

124 For this review, we searched relevant databases, including, Google Scholar, Science Direct, Web of  
 125 Science, to investigate published literature in the past few decades. As indicated by the title, this paper  
 126 focuses on the research and development of the BIPV window. The search keywords were BIPV  
 127 window, crystalline silicon (c-Si), amorphous silicon (a-Si), cadmium telluride (CdTe), copper indium

128 gallium selenide (CIGS), thin-film, Perovskite, dye-sensitized solar cell (DSSC), third-generation PV,  
129 switchable PV, highly insulated BIPV. However, because of the diverse terminology, we also employed  
130 other terms to obtain more work to review which included adaptive, advanced, dynamic, responsive,  
131 and smart window. Windows energetic parameters such as thermal and daylighting properties were  
132 investigated for this work.

133

### 134 **3. Different generation PV based FIPV (BIPV window)**

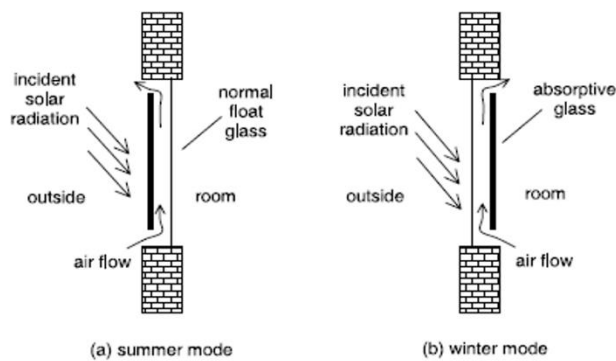
135 Available PV technology for FIPV or BIPV integration includes first-generation crystalline mono and  
136 multi, second-generation thin-film CdTe, CIGS and a-Si and third-generation DSSC, Perovskite and  
137 Organic type. In this section all three generations BIPV windows are evaluated.

#### 138 **3.1. First Generation PV FIPV/BIPV window**

139 Crystalline silicon (c-Si) is the most mature, and highly efficient (27%) technology (Green et al., 2019).  
140 Silicon possesses an energy band gap of 1.12 eV while absorbing solar light up to 1160 nm. Semi-  
141 infinitely thick silicon solar cell has a theoretical conversion efficiency of 33.5% at 25°C (Green,  
142 2005)(Dupré et al., 2015). The mid-infrared emissivity (MIR) of commercial silicon solar cells for an  
143 unencapsulated case is around 80% which is dominated by surface texture and highly doped regions.  
144 The MIR emissivity is 90% for an encapsulated cell due to cover glass high emissivity (Riverola et al.,  
145 2018). Long term durability under extreme outdoor conditions and mature technology make c-Si a  
146 suitable candidate for BIPV application. The price of silicon also reduced from \$475/kg in 2000 to  
147 \$25/kg in 2008 (Fu et al., 2015). From the 2016 level, it is expected that the c-Si PV market will grow  
148 11.3% by 2022 with a market amount of \$163 billion (Luo et al., 2018; Ogbomo et al., 2017). Presently,  
149 Canadian Solar JA Solar, JinkoSolar, Hanwha Q-CELL, LONGI, Tongwei, Trina Solar are the leading  
150 vendor for c-Si PV cells.

151 c-Si based FIPV needs a special arrangement of cells because c-Si PV has 90.5% absorption which  
152 makes it behaves like an opaque system (Santbergen and van Zolingen, 2008). To enable the  
153 transmission through a c-Si PV based FIPV, spaced are given between two cells. For a given area of  
154 glazing depending on the number of PV cells transparency can be varied. Using space between  
155 crystalline PV cells, semi-transparent PV glazing was fabricated using glass, encapsulation material  
156 (Ethylene Vinyl Acetate (EVA), Polyvinyl butyral (PVB), Thermoplastic polyolefin (TPO)), PV cells,  
157 encapsulation material, glass, air gap with spacer and glass. A total of 500 cells, where each cell had  
158 0.127×0.127 m dimensions was connected to form this device. Minimum and maximum power from  
159 these 500 cells were achieved 2.3 W and 2.5 W, respectively. For indoor condition, power decreased  
160 about 0.48% /°C while 0.52% changed for outdoor condition at 500W/m<sup>2</sup> intensity. Solar gain factor,  
161 heat loss and daylighting analysis using this spaced type semi-transparent PV glazing were not included  
162 in this work (Park et al., 2010). c-Si PV based FIPV with a 180-degree reversible mechanism was  
163 proposed by (Chow et al., 2006) as shown in **Figure 2**. In summer, PV will block the unnecessary solar  
164 gain and natural or mechanically driven air flow will go out. Thus, it will reduce cooling energy. In  
165 winter, the opposite phenomenon will occur. Numerical analysis based on Hong Kong climate, potential  
166 of energy saving in summer was high but in winter due to limited period of mild winter, an 180° rotation  
167 was not justified. It was also noted that for summer dominating countries where cold weather never  
168 exists reversible mechanisms may not be necessary. In another work, spaced type, semi-transparent c-  
169 Si BIPV window was employed for skylight application. At Kovilpatti (9°10'0N, 77°52'0E), Tamil  
170 Nadu, an experiment was performed for rooftop window application. Three PV cell coverage were  
171 maintained for three modules and they were 0.62, 0.72, and 0.85. A maximum daylight factor of 4%  
172 and indoor illuminance of 850 lux is obtained in 0.62 (Karthick et al., 2018a). Later temperature  
173 enhancement was reduced using Glauber salt inorganic PCM (Karthick et al., 2018c).

174



176

(a)

(b)

177 Figure 2: (a) Working principle of ventilated solar screen window ((Chow et al., 2006) (b) spaced type  
178 PV glazing in a sunroom at the republic of Korea ((Park et al., 2010))

179 The primary issue with spaced type semi-transparent type FIPV is the presence of tabbing wire which  
180 can create an obstacle to view. Also viewing through this window is not aesthetic. Temperature is an  
181 immense factor for c-Si PV cells. For an unencapsulated c-Si absorption are 90% between 400 nm to  
182 1000 nm and 80% between 1000 nm to 10  $\mu\text{m}$  (Nikolskaia et al., 2019). For an encapsulated c-Si  
183 emissivity in the mid-infrared region is 90% (Santergen and van Zolingen, 2008). Omission of the  
184 highly doped regions and no surface texture Si wafer possess less than 20% emissivity above 1100 nm  
185 (Zhu et al., 2014). The absorption factor of c-Si PV cells depends on the front texture and the metal grid  
186 coverage and is less dependent on the wafer. For c-Si solar cells, every temperature rise of 1 K leads to  
187 a relative efficiency decline of about 0.45% (Skoplaki and Palyvos, 2009a, 2009b).

188

### 189 3.2. Second-generation PV based FIPV

#### 190 3.2.1. Amorphous silicon (a-Si)

191 Amorphous silicon (a-Si) PV works with a much higher efficiency under low illumination compared to  
192 c-Si because of its very high ratio of photo to dark conductivity (Stuckelberger et al., 2017). 25 years  
193 of operation life and 2-3 years of the energy payback time is possible for a-Si (Peng et al., 2013; Zhang  
194 et al., 2018; Zhou and Carbajales-Dale, 2018). According to PV reports developed by Fraunhofer  
195 Institute for Solar Energy Systems, a-Si had a market share of 0.2% in the year 2020. The annual energy  
196 consumption of an office building in Japan having a-Si based FIPV showed that 40% transparent PV  
197 and 50% window-wall ratio achieved the minimum electricity consumption. This FIPV was able to  
198 reduce 55% electricity consumption compared to the single-glazed window without lighting control.  
199 No experiments were performed to support this Energy Plus simulation results (Miyazaki et al., 2005).  
200 In another work, for the cooling load dominated climate, in the Huazhong University of Science and  
201 Technology campus (as shown in **Figure 3**), 20% and 32% transparent single glass a-Si FIPV performed  
202 better than 87% and 71% transparent single and double glazing. However, 62% low-e coated double  
203 glazing performed well compared to FIPV because of the control over NIR transmission (Liao and Xu,  
204 2015). Thermal performance of double-glazed PV showed reduction of 53.5% and 43% solar heat gain  
205 (infrared radiative heat transfer and convective heat transfer) and power generation respectively than  
206 single glazed FIPV in Hefei (31.87° N, 117.27° E), east region of China. Higher thermal comfort was  
207 achieved using double glazing due to lower surface temperature than single glazing (He et al., 2011).

208 In terms of experimental field research, Olivieri et.al. investigated four see-through a-Si BIPV windows  
209 of different transmittances in Madrid and found that the solar protection and insulating properties of a-

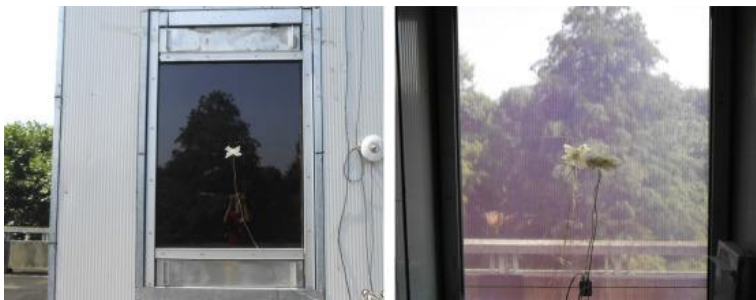
210 Si BIPV windows are lower than those achieved by a reference glazing (traditional glazing) (Olivieri et  
211 al., 2014). Energy performance of a medium-sized office building having 10000 m<sup>2</sup> floor area, 30%  
212 window to wall ratio (total window area 652 m<sup>2</sup>) was investigated for six different climatic conditions  
213 in the USA using three different transparent a-Si based retrofit double-pane glazing. 30% visible  
214 transparent a-Si had 120 nm thick a-Si:H absorber while 14% had 180 nm thick (flat PV cell), 6% had  
215 180 nm thick (textured PV cell) a-Si:H absorber. For semi-arid Los Angeles, CA (34°03N, 118-150W)  
216 thick textured PV cell-based glazing saved annually 34% and 66% cooling and heating energy  
217 compared to 88% transparent (visible) double-pane glazing for this office building (Chae et al., 2014).  
218 Net energy performance of a-Si FIPV (5.497 W/m<sup>2</sup>K, 0.471 SHGC, 15% visible transmittance, 26%  
219 solar transmittance) integrated to an office building in Hong Kong dimension of 2.3 m × 3.0 m and 2.5  
220 m where WWR was 0.41 was investigated using Energy plus software. Results were compared with  
221 single (5.8 W/m<sup>2</sup>K, 0.81 SHGC, 88% luminous transmittance), double (2.68 W/m<sup>2</sup>K, 0.704 SHGC,  
222 78% luminous transmittance) and low-e coated glazing (1.618 W/m<sup>2</sup>K, 0.275 SHGC, 63% luminous  
223 transmittance). This a-Si FIPV saved up to 18%, 16% and 1% electricity energy compared to clear  
224 single glazing, double-pane glazing and Low-E glazing respectively. For south-facing FIPV, total  
225 electricity saving was up to 7% higher than the east-oriented ones (Zhang et al., 2016). Energy analysis  
226 of see-through PV windows in Singapore revealed that optimisation of the window-to-wall ratio with  
227 different design strategies is essential to achieve the maximum energy benefit (Ng et al., 2013). Potential  
228 energy savings by using a-Si based semi-transparent BIPV window for office buildings located at  
229 Fortaleza and Florianopolis which are the two Brazilian cities were evaluated and found this type of  
230 technology is more suited in Brazil than Germany (Leite Didoné and Wagner, 2013).

231 Double glazed ventilated FIPV consists of a semi-transparent a-Si PV at the external surface (a-Si  
232 STPV), an inner layer of glass sheet as well as an intermediate air ventilation cavity. The air outlet and  
233 inlet louvers are installed above and below the PV modules, respectively. This particular type is  
234 lucrative as cold air from the exterior environment exchanges heat from PV and remove waste heat  
235 from a cavity. Thus, PV cells operating temperature reduces, lessens building cooling load, improves  
236 conversion efficiency of PV. Using meteorological weather data of Hong Kong, daylight simulation of  
237 the Energy Plus program showed that PV cell transmittance in the range of 0.45–0.55 best suited for  
238 electricity generation (Chow et al., 2007). In another study, ventilated FIPV having 0.45-0.55  
239 transmittance saved up to 55% energy (Chow et al., 2007).

240 Theoretical models developed via the ESP-r simulation validated results experimentally which showed  
241 that a 23% and 28% reduction in the annual electricity consumption for cooling is possible when single-  
242 glazed and ventilated double-glazed PV windows are used, respectively (Chow et al., 2009). Optimized  
243 air gap for ventilated semi-transparent a-Si DSF was evaluated. It was found that for Berkeley climate  
244 the air gap depth between 400 and 600 mm is beneficial as they save 15% net electricity compared to  
245 the 200 nm thick air gap. In Berkeley, the naturally-ventilated PV-DSF saves about 35% of electricity  
246 use per year than non-ventilated PV-DSF (Peng et al., 2016).

247

248



249

250 Figure 3: See-through a-Si PV glazing (20% visible transmission) in an experimental room at Huazhong  
251 University of Science and Technology, Wuhan, Hubei, China (Liao and Xu, 2015).

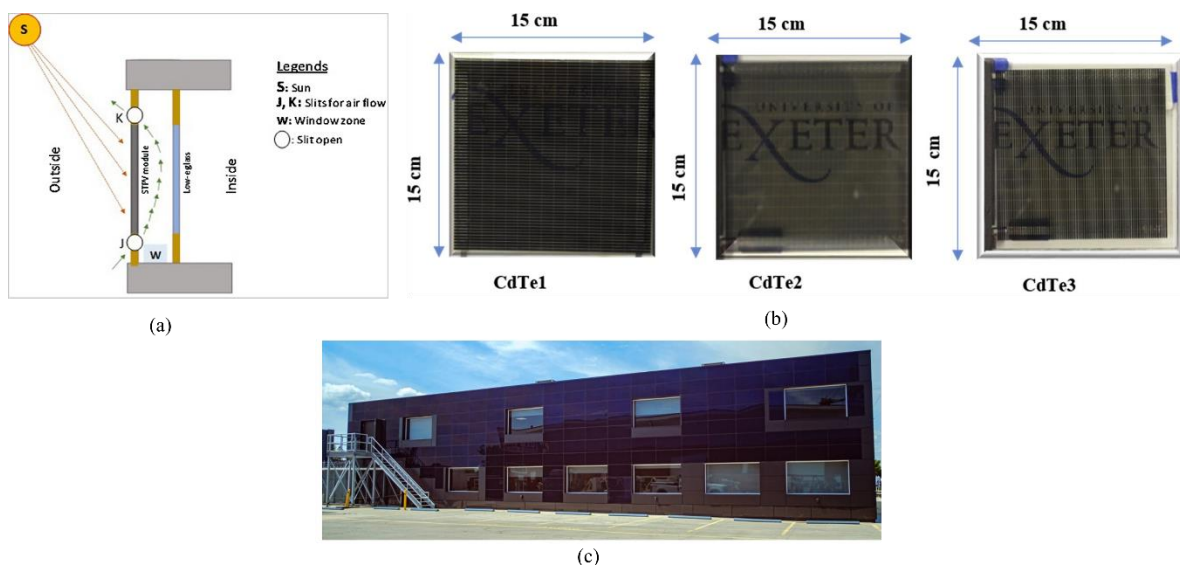
### 252 3.2.2. Cadmium telluride (CdTe)

253 Cadmium telluride (CdTe) PV based FIPV is another option that is currently under major investigation.  
254 According to PV reports developed by Fraunhofer Institute for Solar Energy Systems, CdTe had a  
255 market share of 6.1% in the year 2020. Currently, CdTe has an energy payback time between 0.75 to 2  
256 years and 20 years of operational lifetime (Peng et al., 2013; Zhang et al., 2018; Zhou and Carbajales-  
257 Dale, 2018; Zidane et al., 2019). Cadmium itself is toxic, but not toxic when bound to telluride. CdTe  
258 solar module manufacturer First Solarpanel recently developed a module having 0.2% degradation per  
259 year and  $-0.28\%/^{\circ}\text{C}$  temperature coefficient. This degradation rate is 60% lower than c-Si and is  
260 expected to work efficiently for 30-years (Bellini, 2021).

261 CdTe for FIPV application was performed using EnergyPlus software for a building located at the  
262 Indian city of Jaipur, ( $26.82^{\circ}\text{N}$ ,  $75.8^{\circ}\text{E}$ ) as shown in Figure 4a. Five different luminous transmittance  
263 CdTe (7.0%, 12.3%, 17.7%, 25.2% and 32.7%) were employed for investigation. All these glazings had  
264 a uniform  $U$ -value of  $1.812 \text{ W/m}^2\text{K}$ . SHGC changes for all devices based on the transmittance. It was  
265 found that low increase of cooling load and higher decreased rate of heating load while transparency  
266 increased. In this location with that SPTV system SHGC had a lower impact on building heating and  
267 cooling load. For south-facing, 20% WWR using this CdTe PV was capable to meet the artificial  
268 lighting energy demand however for the east and west larger areas are required (Barman et al., 2018).

269

270



271

272 Figure 4: (a) Schematic of CdTe based air flow FIPV glazing (Barman et al., 2018) (b) Photographs of  
273 three different transparent CdTe PV for BIPV window. (c) Solar Facade System integrated of the  
274 EllisDon offices in London (Image source: Solstex)

275 CdTe FIPV for roof integration was evaluated using EnergyPlus software for five different cities  
276 (Florianópolis, Curitiba, São Paulo, Rio de Janeiro, Brasília Belém) in Brazil. This glass on glass CdTe  
277 PV module had  $122.5 \text{ Wp}$  power, a  $U$ -value of  $5.7 \text{ W/m}^2 \text{ K}$ , a solar heat gain coefficient of 0.35 and a  
278 visible light transmittance of 50%. For Sao Paulo city and a particular building, rooftop and façade  
279 application produced 62% higher energy than the buildings energy demand and excess was  
280 recommended to employ to recharge electric vehicle (Sorgato et al., 2018). Using EnergyPlus, CdTe  
281 FIPV was evaluated for Hong Kong climate. This 10 storied building was designed using the standard

282 Building code for Hongkong while the window to wall ratio was 0.6. Net energy saving potential using  
283 CdTe BIPV window as 15.5% higher than a-Si based BIPV window and 19.6% than a traditional  
284 window. Transmission of a-Si (6%) was lower than CdTe (10%) which increased the lighting energy  
285 demand for a-Si BIPV. For traditional windows the solar heat was higher which was reduced due to the  
286 CdTe integration hence cooling load demand was possible to reduce (Meng et al., 2018). Solar and  
287 luminous light transmission control potential of three 15 cm × 15 cm CdTe based BIPV windows was  
288 evaluated using Indoor spectral characterisation as shown in **Figure 4b**. Three different CdTe glazing  
289 systems were 5.77% (CdTe1), 9.54% (CdTe2) and 12.34% (CdTe3). Spectral behaviour of reflections  
290 in the range of solar and visible wavelengths was similar for these three different transparent CdTe  
291 glazing. Near infrared (NIR) reflection was higher compared to luminous reflection after 1500 nm for  
292 all three glazing systems. Solar factor (SF) for CdTe1, CdTe2 and CdTe3 glazing were 0.23, 0.28, and  
293 0.26. CdTe3 is the best candidate for glazing application as it has 113% higher luminous transmission  
294 while SF only increases by 21% compared to CdTe1 (Alrashidi et al., 2019). *U*-value and *g*-value of  
295 semi-transparent CdTe FIPV were experimentally characterised at temperate climate which confirmed  
296 that 25% visible transmission and 12% solar transmission. Thermal transmission and solar heat gain  
297 coefficient were calculated from measured thermal data. *U*-value of 2.7 W/m<sup>2</sup> K was found for outdoor  
298 and indoor characterization of CdTe BIPV windows (Alrashidi et al., 2020a). Façade buildings are  
299 generally highly glazed and energy-intensive especially in countries with hot weather. Power  
300 consumption in these buildings is even more significant when the air conditioning (AC) is added to the  
301 figures. Building with semi-transparent photovoltaic (STPV) materials is bringing advantageous  
302 energy-saving features to these façade structures. Energy is saved by more heat being reflected resulting  
303 in less AC power consumption with the STPV thermal properties. In addition, the optical and electrical  
304 properties provide indoor sunlight with power generation. This paper investigates the net potential  
305 energy-saving via applying cadmium telluride (CdTe) in Façade buildings. The analysis has been  
306 carried out using indoor and outdoor experiments considering different orientations and transparencies.  
307 Compared to a single glazing case as a reference, the applied CdTe achieved a net energy saving of  
308 20%. Furthermore, a trade-off between saving energy and environmental comfort has been discussed  
309 as less transparency windows lead to more artificial light consumption. The findings indicate that STPV  
310 is a promising solution for sustainable buildings (Alrashidi et al., 2020b). Daylighting performance  
311 using CdTe FIPV (10% to 50% transparent) was evaluated by employing UDI, DGPs, Uniformity ratio  
312 (Sun et al., 2020). It was found that even a 10% transparent CdTe BIPV window can produce UDI  
313 levels 500 to 2000 lux. **Figure 4c** shows a solar facade system integrated into the EllisDon offices in  
314 London.

### 315 **3.3.3. Copper, indium, gallium and selenium (CIGS)**

316 Copper, indium, gallium and selenium (CIGS) thin-film solar cells are another promising thin-film  
317 technology that can be employed as FIPV. In this type of structure, on glass or flexible substrate, thin-  
318 film, the buffer layer and transparent upper electrode are coated. Due to low-cost fabrication methods  
319 compared to c-Si solar cell CIGS gaining importance (Mufti et al., 2020). Compared to CdTe this is not  
320 toxic. Because of the lack of highly efficient cells, this technology is still yet not very commercially  
321 popular. For large-scale deployment of CIGS, Indium is not a limiting factor (source: PV magazine).  
322 Recently, 23.35% record efficiency was achieved by Japanese manufacturer Solar Frontier for a CIGS  
323 solar cell and 19.64% efficiency was recorded for a CIGS module by German thin-film module maker  
324 Avancis. Potential of CIGS-BIPV for energy saving and environmental protection, economic,  
325 innovation and safety shows it can score high enough (86/100) which make it competitive compared to  
326 other commercial product (Kong et al., 2020). However to capture the global market, low price, better  
327 quality and low user costs are also essential in addition to high efficiency. According to PV reports  
328 developed by Fraunhofer Institute for Solar Energy Systems, CIGS had a market share of 1.5% in the  
329 year 2020.

330



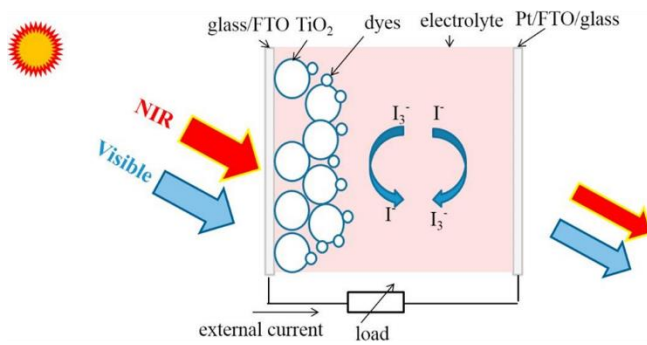
331

### 332 3.3. Third-generation PV based FIPV

#### 333 3.3.1. Dye-sensitized solar cell (DSSC)

334 Dye-sensitized solar cells (DSSC) is potential for FIPV application due to their, transparency, low-cost  
335 fabrication process, eco-friendly property (Gong et al., 2012). The energy payback period of DSSC  
336 varies from 1.99 years to 2.63 for varying cell efficiency (Greijer et al., 2001; Mustafa et al., 2019;  
337 Parisi et al., 2014, 2011). The market value of DSSC is expected to be USD 49.6 million in 2014 and  
338 is estimated to grow at a CAGR of over 12% from 2015 to 2022. In the presence of sunlight radiation  
339 dyes of DSSC degrades. The use of liquid electrolytes leads to leakage problems it may expand at high  
340 temperature and freeze at low temperature (Richhariya et al., 2017). Solid electrolyte based DSSC is in  
341 research nowadays. **Figure 5a** shows the schematic of DSSC while **Figure 5b** shows the LSC window  
342 at Hanbat National University, Daejeon, in the Republic of Korea and **Figure 5c** shows the LCS window  
343 at EPFL.

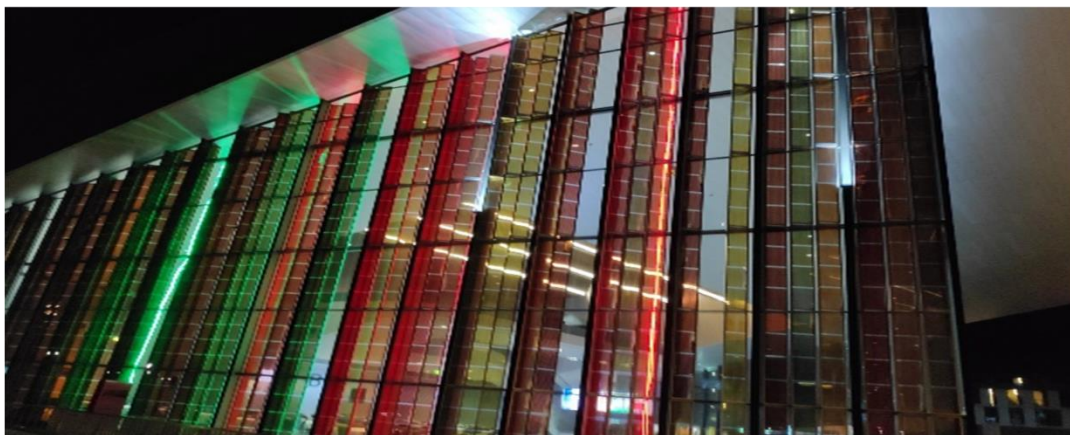
344



(a)



(b)



(c)

345

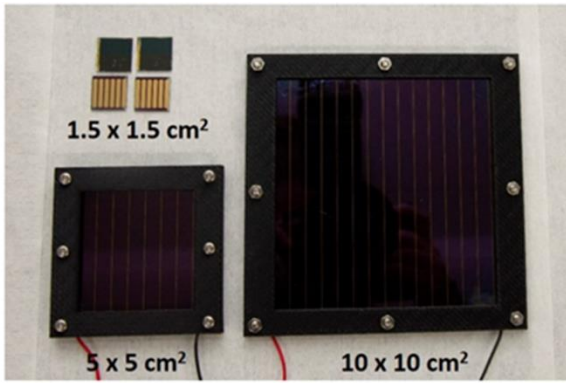
346 Figure 5: (a) Schematic of DSSC, (b) 4 vertically placed DSSC module 81.36 Wp (each module has  
347 20.34 Wp) at Hanbat National University, Daejeon, in Republic of Korea (Lee and Yoon, 2018), (c)  
348 LSC window at EPFL.

349 One DSSC for FIPV application was designed by a nine-unit solar cell connected in series. One unit  
350 cell had  $80 \times 80 \text{ mm}^2$  active areas, 8 mm thick  $\text{TiO}_2$  layer, open-circuit voltage of 0.64V, short circuit  
351 current of 250 mA. This FIPV generated  $V_{oc}$  of 5.7 V and  $J_{sc}$  of 220 mA at one sun light intensity.  
352 This DSSC glazing had an average of 60% transmission in the visible and a maximum of 67%  
353 transmission at 670 nm. However, no thermal or energy performance was performed using this glazing  
354 (Kang et al., 2003). In another work, 7  $\mu\text{m}$ , 9  $\mu\text{m}$  and 11  $\mu\text{m}$  thick  $\text{TiO}_2$  and red and green coloured dye-  
355 based total six DSSCs were fabricated to investigate their optical and thermal performance using  
356 Window 6 software. Unit cell dimension was  $10 \text{ mm} \times 10 \text{ mm} \times 4.5 \text{ mm}$ . The average transmission of  
357 these cells was greatly influenced by the thickness of the material and varied from 6% to 30% in the  
358 visible range. Average 27% visible transmission DSSC glazing offered 0.29 SHGC whereas 0.78  
359 transmitted double glazing offered 0.71 (Kang et al., 2013). Varying  $\text{TiO}_2$  thickness, four different  
360 transparent DSSCs were fabricated. This 39%, 31%, 24% and 20% luminous transparent DSSC glazing  
361 had conversion efficiencies of 10.26%, 11.50%, 12.60%, 13.00% respectively. The higher thickness of  
362  $\text{TiO}_2$  offered low transmission and high power conversion due to higher short circuit current from a  
363 thicker electrode. Using these DSSC glazing, the energy performance of a building in Korea was  
364 evaluated by using energy simulation techniques. Without DSSC glazing showed that lower  
365 transmission enhanced energy consumption due to heating load requirement where as DSSC showed  
366 reverse as it generated electricity (Yoon et al., 2011). The  $U$ -value of these four-glazing varied from  
367 1.49 to 1.53  $\text{W/m}^2\text{K}$ . To achieve a lower  $U$ -value a combined system was considered where this DSSC  
368 glazing was external surface and one low-e coated glass was placed between this DSSC glazed pane  
369 and clear pane. New overall  $U$ -value varied from 0.79-0.84  $\text{W/m}^2\text{K}$  while SHGC of 0.2, 0.19, 0.17 and  
370 0.15, respectively. Using ESP-r program building energy performance for integration of this glazing  
371 was simulated for seven different cities (Miami, Sao Paulo, Sydney, New York, Seoul, Berlin, and  
372 Moscow). This glazing was performed best in New York City due to its variable heating and cooling  
373 load demand. For cooling dominant Berlin and Moscow climate, the glazing performance was less  
374 effective (Lee et al., 2014). DSSC integrated between glass block ( $U$ -value of 3.0  $\text{W/m}^2\text{K}$ , solar factor  
375 79.7% and 79.5% light transmission) were investigated at the University of Palermo. COMSOL  
376 Multiphysics, WINDOW, Zemax were employed to explore the thermal, optical and electrical  
377 performance (Morini and Corrao, 2017). On other work, 5 different DSSC glazing including opaque  
378 green, transparent green, opaque red, transparent red, double glazing red having a dimension of 60 cm  
379  $\times$  100 cm was selected. Because of the low visible transmittance, it was advised to employ half of the  
380 façade (Bouvard et al., 2015). Varying  $\text{TiO}_2$  electrode thickness six small-scale DSSC based FIPV were  
381 fabricated which offered luminous transmittance between 0.19 and 0.53. Evaluation of the colour  
382 rendering index (CRI) and correlated colour temperature (CCT) of below 0.5 transmittances showed a  
383 CRI lower than 80. Interestingly, the CRI of 53% transparent DSSC glazing had only 2.7% lower CRI  
384 than 77% transparent double glazing and 72% transparent vacuum glazing (Ghosh et al., 2018b). It is  
385 found that the 37% transparent DSSC FIPV reduced 21% disturbing glare than a traditional double  
386 glazed window for a clear sunny day in a temperate climate (Selvaraj et al., 2019). After two years the  
387 same device showed that though average visible transmission reduced, colour properties were enhanced  
388 for them which is essential properties for FIPV (Roy et al., 2019). First outdoor characterisation of  
389 DSSC FIPV to understand long term performance was carried out employing 20.34 Wp, 0.975 m  
390 (W)  $\times$  0.965 m (H) system at Hanbat National University, Daejeon, Republic of Korea. The structure  
391 had DSSC module (9 mm)” + “air space (12 mm)” + “clear glass (5 mm)”. Results were compared with  
392 40° sloped DSSC FIPV. Power yield of sloped DSSC was higher because DSSC is reactive with diffuse  
393 solar radiation than direct solar radiation (Lee and Yoon, 2018).

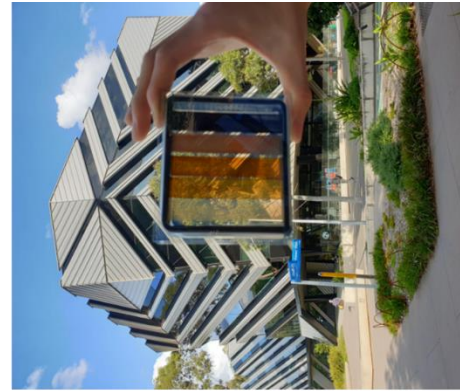
### 394 3.3.2. Perovskite

395 Perovskite solar cells (PSC) possess tuneable transparency and simpler fabrication methods and gained  
396 efficiency from 3% to 22% within a decade which most trending technology for FIPV application.  
397 Currently, the highest efficiency of single-junction PSC has reached 25.5% (Green et al., 2020).  
398 Perovskite's energy payback analysis is not a much-explored area, however, few works suggested that  
399 it can be between 0.2 to 5 years depending on the employed material. Depending on the module  
400 efficiency the LCOE also varies. It was evaluated that the LCOE of a perovskite-based PV module can  
401 have a cost of 0.25 US\$/W for 15 years of a lifetime. For varying module efficiency such as  
402 12%,15%,20%, the LCOEs were 4.9 US cents/kWh, 4.2 US cents/kWh, and 3.5 US cents/kWh  
403 respectively (Cai et al., 2017). It is expected that by 2022 the global Perovskite PV market will be \$5.2  
404 billion by 2022 (Research, 2018). Oxford photovoltaics, OIST's Technology, Solliance, Toshiba and  
405 NEDO are currently the major Perovskite PV cell developer (Roy et al., 2020).

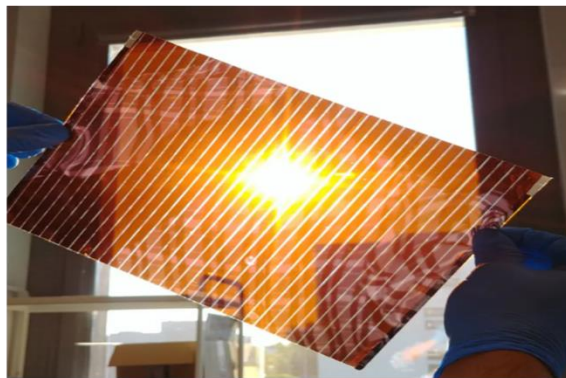
406 Long term device stability is one of the most imperative challenges for the emerging PSC technology.  
407 Moisture, oxygen, temperature, and illumination are the four key elements that degrade the PSC.  
408 Although encouraging ageing results have been reported at milder or controlled environmental  
409 conditions, still, there is a long way to go to meet stability standards similar to thin-film PV technology  
410 (IEC 61646) and crystalline silicon PV technology (IEC 61215). Especially, no promising results have  
411 been reported yet for heat damp test (85 °C, 85 RH) and light soaking tests at 85 °C. Passing the IEC  
412 61215 is necessary for Perovskite to clear the minimum requirement for commercialisation (Holzhey  
413 and Saliba, 2018). Both the materials and their preparation methods have been found to influence the  
414 device stability (Asghar et al., 2017). Large scale fabrication of PSC is challenging because it's hard to  
415 produce a large uniform layer of perovskite as defects become more pronounced which can only be  
416 solved by increasing the film thickness. However, higher thickness reduces the transmission property.  
417 Recently, Perovskites modules having dimensions of 5 cm × 5 cm and 10 cm × 10 cm, with efficiencies  
418 of 14.55% and 10.25% were developed as shown in **Figure 6a**, which performed well for 1,600 hours  
419 maintaining 80% of its standard efficiency while the larger module maintained its 10.25% efficiency  
420 for over 1,100 hours (Tong et al., 2021). Spiro-OMeTAD-free ST-PeSCs in normal type devices were  
421 achieved at AVT values between 10 and 30% as shown in Figure 6b (Choul et al., 2020). Figure 6c  
422 shows the semi-transparent perovskite made by Saule technologies.



(a)



(b)



(c)



(d)

423

424

425 Figure 6: The two mini solar modules developed by Korean researchers. Image: Okinawa Institute of  
 426 Science and Technology Graduate University (OIST). (b) A semi-transparent perovskite solar cell with  
 427 contrasting levels of light transparency. Source: Dr Jae Choul Yu (Choul et al., 2020), (c) A4 size  
 428 semi-transparent Perovskite by Saule technologies (d) Photograph of semi-transparent Perovskite solar  
 429 cell (Wang et al., 2020)

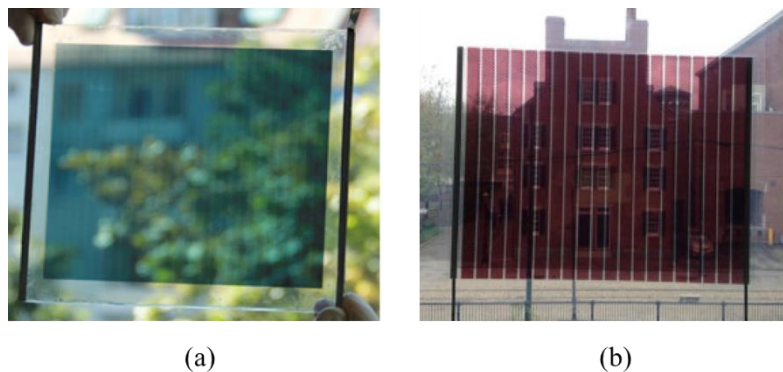
430 Perovskite PV use toxic lead (Pb) which can create a negative impact on users and can be an obstacle  
 431 for its market acceptance. Two types of corrective measures (a) replacing lead with other similar  
 432 properties metal, (b) use of less toxic material could improve the situation. However, it is believed that  
 433 the amount of lead used in PSCs is not significant compared to lead used in lead-cadmium batteries,  
 434 integrated circuits, infrared detectors. PSC uses only  $0.4 \text{ g/m}^2$  of Pb, which is comparatively much lesser  
 435 than the lead used in soldering of commercial Si PV panels (M. Chen et al., 2019). On the other hand,  
 436 completely getting rid of Lead is not a possibility as the performance of lead-free PSCs are still lagging  
 437 behind the lead-based PSCs. The FIPV based on perovskite was reported by (Cannavale et al., 2017).  
 438 In this work, perovskite was prepared by FTO/glass substrate, coating of  $\text{TiO}_2$  n-type layer, deposition  
 439 of dewetted perovskite islands. This particular type of perovskite had an array of perovskite  
 440 microstructure islands and each island absorbed visible light while the transparent region was colour  
 441 neutral (Eperon et al., 2014a, 2014b). This cell had an active area of  $0.0929 \text{ cm}^2$ , FF, conversion  
 442 efficiency was 0.65 and 6.64% respectively (Eperon et al., 2014b). The color perception of transmitted  
 443 light through this 42.4% transparent cell was neutral. Using Matlab and Daysim software, these data  
 444 were applied as input to investigate the glare control potential and energy analysis of perovskite FIPV  
 445 based building. Maximum power conversion reduction was only 3% in hot climates whereas no  
 446 reduction was noticed in colder climates which implied that transparent perovskite absorbs less radiative  
 447 heat. Thus efficiency reduction is less due to temperature (Cannavale et al., 2017). Carbon counter

448 electrode-based Perovskite was developed and experimentally and analytically investigated to  
449 understand its behaviour as FIPV or BIPV window application. At 1000 W/m<sup>2</sup> solar radiation condition,  
450 this Perovskite had 8.13% efficiency while visible and solar average transmittance was 20% and 30%  
451 respectively. Angular incident angel dependent solar heat gain coefficient (SHGC) or solar factor (SF)  
452 varied from 0.14 to 0.33 for the University of Exeter, Penryn (50.16° N, 5.10° W) UK location. *U*-value  
453 was 5.6 W/m<sup>2</sup>K while colour properties analysis found that 20% visible transmittance is the threshold  
454 limit, to obtain colour or visual comfort using this glazing (Ghosh et al., 2020). EnergyPlus simulation  
455 with an advanced FIPV having semi-transparent Perovskite and nanophotonic multilayer coating  
456 showed that 13560 kWh energy saving potential of a single story building (residential 2000 ft<sup>2</sup> area)  
457 which was located at Pheonix, Arizona (shown in **Figure 6d**) (Wang et al., 2020). Recently semi-  
458 transparent Perovskite visual impact for different Kopean climate based location was explored which  
459 indicates the positive future potential of this technology for FIPV application (Bhandari et al., 2022).

460

### 461 3.3.3. Organic

462 Made with no toxic material, lightweight semi-transparent organic solar cells (OSCs) are another  
463 alternative to FIPV application. Long term durability at outdoor conditions is a critical issue with  
464 organic PV based FIPV. Outdoor stability of organic PV (OPV) system having 35.5 cm<sup>2</sup> active area  
465 was performed at 3 different locations in Germany, one in Israel, one in Denmark and one in Australia.  
466 Stability was retained for 17<sup>th</sup> months (Gevorgyan et al., 2013). It was suggested that efficient terminal  
467 sealing is essential to limit the stability issue. Eight different OPV systems degradation was evaluated  
468 at the outdoor condition for 8 months (Owens et al., 2016). OPV has a lower thermal coefficient  
469 compared to c-Si and thin film as it absorbs a lower amount of infrared than the other two (Bristow and  
470 Kettle, 2018). Outdoor characterisation of OPV system at Japan climate showed three types of  
471 degradation which included initial rapid degradation, secondary gradual degradation, and seasonal  
472 variation (Sato et al., 2019). Lucera et.al. 2017 developed 197.40 cm<sup>2</sup> active area based semi-transparent  
473 Organic PV based FIPV which achieved 4.8% efficiencies on rigid substrates (FTO) and 4.3% on a  
474 flexible substrate (ITO-Metal-ITO (IMI) sputtered polyethylene terephthalate (PET)). Details of  
475 transmission and other window parameters were not evaluated. **Figure 7** shows two different types of  
476 organic solar cell based FIPV.



477

478 Figure 7: (a) Green like with active area of 197.40 cm<sup>2</sup> (Lucera et al., 2017) (b) Red like (Yan et al.,  
479 2013) semi-transparent Organic FIPV

480 In another work, semi-transparent organic PV based FIPV was developed which had 3% efficiency and  
481 after accelerated durability test following IEC 61646:2008 only 8% degradation occurred (Yan et al.,  
482 2013). Organic FIPV for greenhouse shading in Israel for agriculture purposes was investigated which  
483 had 20% transmission, 15% reflection and absorption was 65% absorption. This system also had a *U*-  
484 value of 6.0 W/m<sup>2</sup>K (Friman et al., 2019). The cost of organic FIPV is lower than the first generation  
485 as roll to roll technology can be employed here. Also, the temperature coefficients are positive for OPV

486 BIPV. Table 1 lists here the difference between three different generations of PVs for the BIPV window  
 487 or FIPV application.

488 Table 1: Comparative analysis of three different generations of PV for BIPV window application.

Type	Solar cell type	Transparency	Current highest efficiency	Stability	Temperature impact/temp. coefficient (K <sup>-1</sup> )	BIPV window application
1 <sup>st</sup> Generation						
	Silicon (Si)	Opaque	26.7%	Mature technology 20-25 years working capacity	High-temperature power reduces/ -0.2 to -0.45 (Skoplaki and Palyvos, 2009a, 2009b)	Spaced type structure is possible
2 <sup>nd</sup> Generation	a-Si	Opaque, Semi-transparent	10.2%	Mature technology 20-25 years working capacity,	Wekaer effect than Si/ -0.10 to -0.30	possible
	CdTe	Opaque, Semi-transparent	21%	Mature technology Expected to work over 20-25 years, however no such work is reported yet	Wekaer effect than Si/ -0.25 and (Lee and Ebong, 2017)	possible
	CIGS	Opaque, Semi-transparent	23.35%	Partially mature technology, Expected to work over 10 years however no such real work is reported yet	Wekaer effect than Si/ -0.33 to -0.50 (Virtuani et al., 2010)(Deceglie et al., 2014)	possible
3 <sup>rd</sup> Generation	DSSC	Opaque, Semi-transparent, transparent	11.9%	Stability with high efficiency is still challenging issues	+0.1 (30°C-50°C)  (Tian et al., 2012)	possible
	Perovskite	Opaque, Semi-	22.6%	Not stable at outdoor environment	a) 0.035 between	possible

	transparent, transparent			5°C and 25°C	
				b) -0.021 between 25°C and 75°C (Bhandari et al., 2020)	
Organic	Opaque, Semi- transparent, transparent	15.2%	Life span maximum 4-5 years	+0.7	possible

489

490

491 **4. Advanced FIPV/BIPV window**

492 **4.1. Concentrating PV based FIPV**

493 The use of environmentally benign materials based concentrators replace the costly PV material with  
 494 low cost concentrating material, generates higher electrical power, abate the use of toxic material during  
 495 PV cells production. Concentrator includes a high, low, and medium type. Concentrator below 10 is  
 496 considered as low while between 10 to 100 is medium and above 100 is high. For high and medium,  
 497 cooling agent is required while for low natural air flow can reduce the thermal enhancement. For  
 498 building applications, a low concentrator is popular.

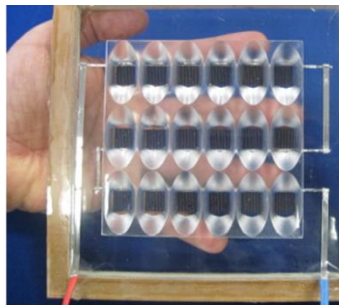
499

500

501



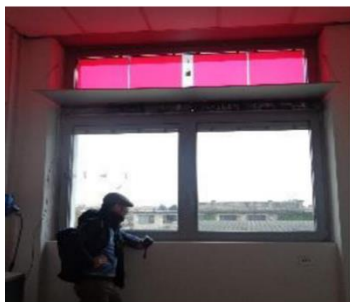
(a)



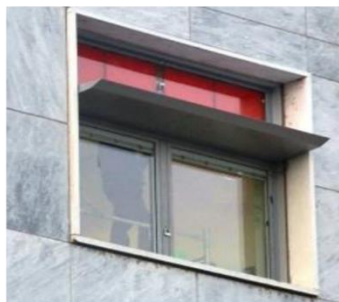
(b)



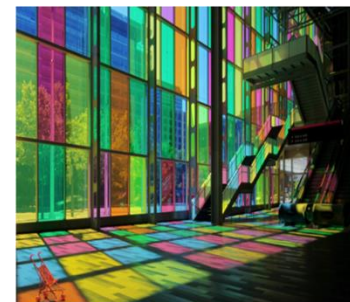
(c)



(d)



(e)



(f)

502

503 Figure 8: (a) BICPV window at the University of Exeter, Penryn Campus (b) Semi transparency effect  
504 of the square elliptical hyperboloid concentrator for BIPV window application (taken from (Sellami et  
505 al., 2012) (c) Solar squared (Image courtesy Build Solar (taken with permission)), (d) red LSC window  
506 installed in building internal view (Aste et al., 2017) and (e) external view (Aste et al., 2017), (f) LCS  
507 window (Interior view of the Palais des Congrès, Montreal, Canada (photo courtesy M.Nguyen)).

508 Low concentrator for FIPV application includes compound parabolic concentrator (CPC) (Liu and Wu,  
509 2021), luminescent solar concentrator (LSC) and holographic solar concentrator. Mirror-based or  
510 dielectric-filled compound symmetric asymmetric parabolic concentrator's non-imaging nature, this  
511 type of concentrator can collect both direct and diffuse solar radiation. For CPC, mostly c-Si solar cells  
512 are employed and CPC is placed on the top of the PV (shown in [Figure 8 a and b](#)). To allow sufficient  
513 light and view this structure is very much similar to c-Si based FIPV (Li et al., 2020). The only  
514 advantage is the power generation is high and the overall system cost is low as less solar cells are used.  
515 However, other types of solar cells such as DSSC (Selvaraj et al., 2018 and Perovskite (Baig et al.,  
516 2020) were recently used to understand the impact of high light intensity on the cell material. BuildSolar  
517 is now the only commercial player for CPC based FIPV as shown in **Figure 8c**.

518 Luminescent solar concentrator (LSC) as shown in **Figure 8 d,e,f** is another alternative for FIPV  
519 application that harvests both diffuse and direct sunlight. An LSC consists of a transparent polymer  
520 sheet or film, doped with either organic dyes, quantum dot or rare-earth material which absorb a portion  
521 of the incident solar light and emit photons with a near-unity quantum yield. If the refractive index of  
522 the carrier material is higher than that of the surrounding medium (in this context, air), a large proportion  
523 of the emitted photons will reach the edges following total internal reflection. LSCs are less sensitive  
524 to their orientation angle compared to silicon PV modules (Aste et al., 2017). Because of the presence  
525 of solar cells at the edge of the LSC, no special arrangements are required compared to CPC based  
526 FIPV. LCS types FIPV can be different coloured depending on the presence of dyes hence transmission  
527 modulation is possible and thus the daylight control and limiting are also possible.

528

#### 529 [4.2. Bi-facial solar cell-based FIPV](#)

530

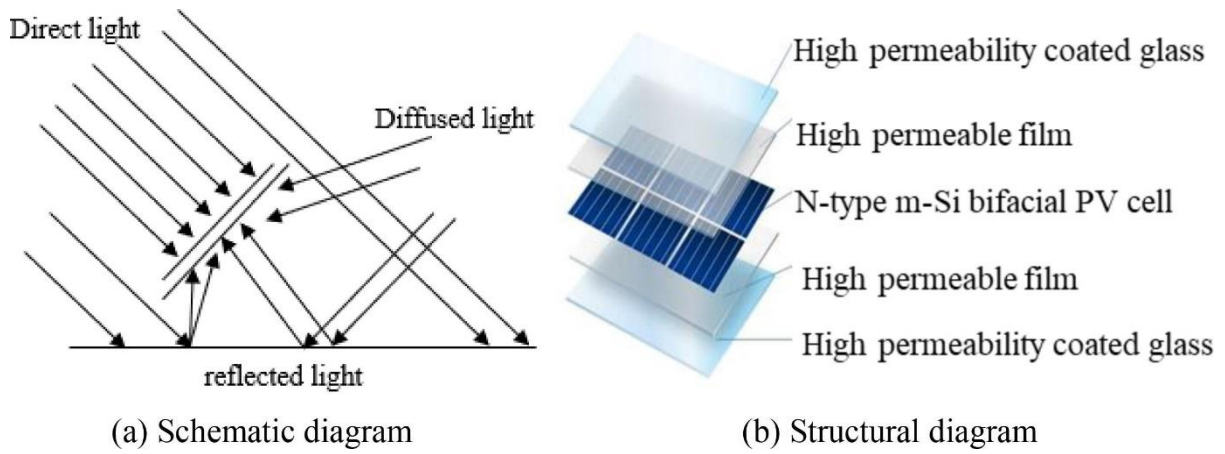
531 Bifacial solar PV collects solar light from both front and back faces which enhances the energy  
532 generation than that of the same footprint as monofacial modules as shown in **Figure 9**. Though it was  
533 developed first in 1960 but had to wait before making its further accelerated innovation (Guerrero-  
534 lemus et al., 2016). In 1984, the first industrial production of bifacial PV (bPV) module was developed  
535 by ISO-FOTON which is a Spanish company (Lorenzo, 2021). As bPV collects higher solar light, it  
536 can be considered that the temperature of the cell can be higher than monofacial one. However, because  
537 of the structure of the bPV module, most of the infrared light transmitted through the system makes its  
538 temperature rise low (Lamers et al., 2018). Thus, glass-glass structure-based bPV can have higher  
539 LCOE than a traditional glass-back sheet and the rear glass is better to withstand the exposed UV rays  
540 and water vapour intrusion (Gu et al., 2020). Because of the low-temperature coefficient of bPV, energy  
541 yield is 20-40% higher than monofacial (Al-BSF) structure (Patel et al., 2020).

542 In general, building integration of the PV module is interesting because of its low degradation due to  
543 the bird droppings, dust, snow, tree leaves. Although it can have a large collection area but suffer from  
544 non-optimal orientation. bPV can be a solution as the gap between the inner wall and module allows  
545 rear side albedo and forced or natural air circulation to reduce the cell temperature. It can be  
546 advantageous seasonally as can allow penetration of heat during winter and vertical shading in summer  
547 (Soria et al., 2016). Power generation from the rear side of the PV from a bPV depends highly on the  
548 building exterior materials which can be various different materials (Russell et al., 2017; Soria et al.,  
549 2016). Also, the distance between this exterior wall which can act as a reflector is not often constant



550 because of the protruded and/or sunken exterior features of buildings (Deline et al., 2020). This  
 551 inhomogeneous rear surface has an adverse impact on the reliability and power generation from bPV  
 552 (Kim et al., 2021).

553



554

555

556 Figure 9: (a) Schematic (b) structural diagram of bifacial PV cells.(Chen et al., 2021)

557

#### 558 4.3. Thermally insulated FIPV

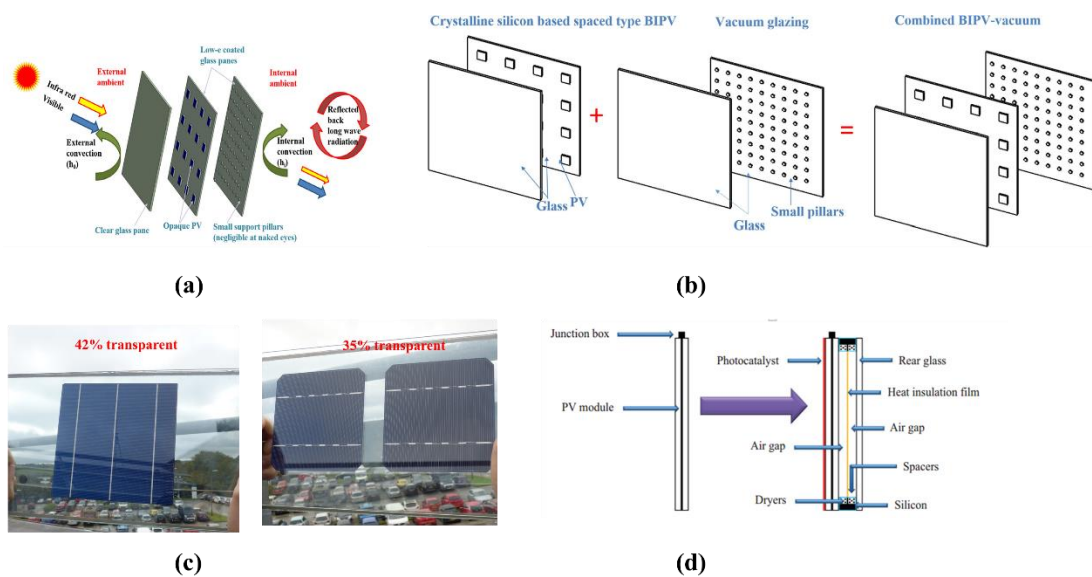
559

560 In general, a BIPV window or FIPV is two glass panes where PV material is sandwiched between two  
 561 glass panes. While because of PV material different transparency, solar factor varies however, the  $U$ -  
 562 value remain similar to double glazing. If there is no space between two glass panes, then overall the  
 563 system works as single glazing. Single glazing possesses a higher  $U$ -value which enhances the building  
 564 heat energy demand. Hence, double, and single glazing are not suitable for cold climatic building  
 565 integration. To enable a glazing system in cold climate building, evacuated (vacuum) glazing is now in  
 566 research interest. Evacuated glazing consists of two glass panes and a vacuum is maintained between  
 567 these two glasses. To withstand outside atmospheric pressure small support pillars are there which  
 568 might be stainless steel or aerogel made. Vacuum glazing has a  $U$ -value close to or lower than  $1 \text{ W/m}^2\text{K}$   
 569 (Fang et al., 2014) and 53% lower heat loss potential compared to double glazing (Ghosh et al., 2016a).  
 570 The presence of vacuum, conduction and convection losses are reduced while the presence of low  
 571 emission coating abates the radiative heat transfer (Memon et al., 2019). Support pillars are most often  
 572 stainless steel (Wilson et al., 1998) (Collins et al., 1995; Griffiths et al., 1998) made while recently  
 573 transparent support pillar made from Bismuth boron glass powder (Zhao et al., 2013), translucent  
 574 aerogel (Büttner et al., 2019) were also investigated. Edge sealing is a critical task for vacuum glazing  
 575 to maintain the low pressure between glasses for the high durability of the system. Solder glass (Collins  
 576 and Robinson, 1991), indium alloy (Zhao et al., 2007), Cerasolzer type CS186 (Memon et al., 2015)  
 577 based edge sealing was investigated for vacuum glazing. Hence, the BIPV-vacuum glazing window is  
 578 the most advantageous for cold climates. C-Si PV based Vacuum integrated FIPV glazing (**shown in**  
 579 **Figure 10 a, b and c**) was reported where indoor test cell characterisation found an overall heat transfer  
 580 coefficient ( $U$ -value) of  $0.8 \text{ W/m}^2\text{K}$  and solar factor of 0.42. Results were compared with a similar area  
 581 of double glass pane based FIPV. Vacuum based system had a 66% lower  $U$ - value and 42% lower  
 582 solar factor than a double glazing-based system. Also, for the cold climate, this vacuum-based system  
 583 is a suitable candidate as lower ambient temperature can abate the enhancement of PV cell temperature  
 584 (Ghosh et al., 2018c). Thermal comfort analysis reported that for a clear sunny day soothing or

585 comfortable indoor temperature is possible during mid-day. For a combined BIPV-vacuum glazing,  
 586 vacuum glass facing external ambient is suitable for cold climate and warm climate vacuum glass facing  
 587 internal room ambient is applicable (Ghosh et al., 2019a). Another work reported that 35% and 42%  
 588 transparent vacuum-based PV windows possess comfortable CCT and CRI for building interior (Ghosh  
 589 et al., 2019b).

590 a-Si based vacuum-based 20% transparent FIPV having a dimension of 1300 mm (width) ×1100 mm  
 591 (height) × 20.87 mm (thickness) was characterised at The Hong Kong Polytechnic University from June  
 592 2016. The U-value of this system was 1.5 W/m<sup>2</sup>K (Qiu et al., 2019). Power output from this system was  
 593 linearly correlated with incident solar radiation (Zhang et al., 2017). Employing Energy Plus simulation  
 594 for two different locations in Hong Kong and Herbin showed a reduction of 81.63% and 75.03% of the  
 595 heat gain while 31.94% and 32.03% respectively. This work also confirmed that vacuum-based FIPV  
 596 is suitable for cold climate areas (Huang et al., 2018). Highly insulated solar glass made by a-Si PV was  
 597 experimentally characterised in the Institute of Sustainable Energy Technologies at the University of  
 598 Nottingham as shown in **Figure 10 d**. This glazing had 79% absorption, 7% visible transmittance, 100%  
 599 UV blockage, 95% restriction of undesired thermal radiation, 24.9% better daylighting performance  
 600 compared to ordinary glazing while U-value was 1.10 W/m<sup>2</sup>K (Cuce et al., 2015a, 2015b). The presence  
 601 of photocatalyst TiO<sub>2</sub> on the glazing surface allows self-cleaning as pollutants on the glazing surface  
 602 are decomposed by photocatalysts and will be washed away during rain. These layers also offer high  
 603 transmittance and low reflection. Semi-transparent thin-film PV insulated with vacuum layer-based  
 604 FIPV was investigated theoretically where support pillar was aerogel made and edge sealing was epoxy  
 605 resin type to reduce the overall weight and conductive heat transfer of the window. COMSOL  
 606 Multiphysics was employed to evaluate the U-value of the system which was 0.3255 W/m<sup>2</sup>K (B. Chen  
 607 et al., 2019). Aerogel support pillars have the ability to reduce 20% of U- value compared to stainless  
 608 steel as the support pillars (Jarimi et al., 2020). To lower the U-value further for BIPV-vacuum glazing  
 609 an intermediate air cavity between PV and vacuum glazing was theoretically investigated. The three-  
 610 dimensional heat transfer model showed that this PV-vacuum-double glazing window can achieve a  
 611 0.23 W/m<sup>2</sup>K U-value while PV side faced cold outdoor environment and vacuum glazing facing indoor  
 612 environment, an air cavity is 12 mm and pillar spacing is 60 mm (Huang et al., 2021).

613



614

615 Figure 10: (a) and (b) schematic of spaced type semi-transparent vacuum FIPV glazing (Ghosh et al.,  
 616 2018c), (c) photographs of BIPV- vacuum glazing (Ghosh et al., 2019b), (d) Schematic of highly  
 617 insulated FIPV glazing (Cuce et al., 2015) and

618

#### 619 4.4. Switchable BIPV

620

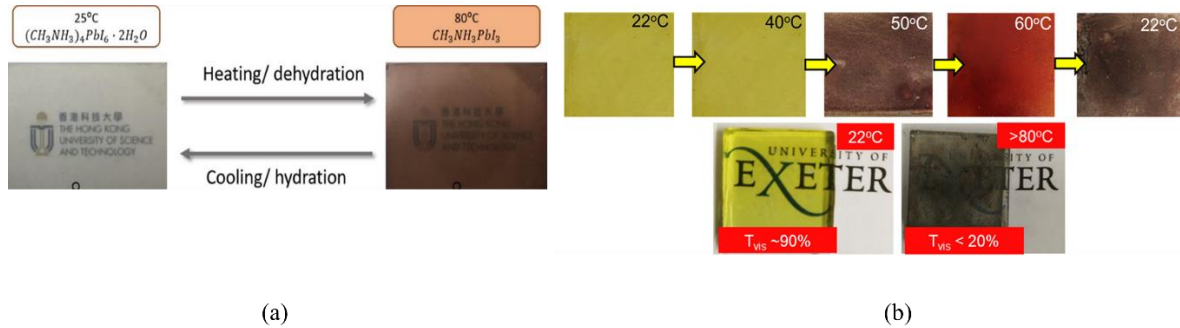
621 Currently, static or constant semi-transparent PV dominates the BIPV window sector, which  
622 concomitantly provides power and shading. However, they are incapable to change the transmission  
623 similar to a smart window, which can alter their transmission by employing some external stimuli. It is  
624 highly desirable to develop the material, which can have the potential to generate electricity in an  
625 opaque state and allow light transmission in the transparent state while both states are switchable and  
626 stable under external ambient. Perovskite material has the ability to change the transparency in the  
627 presence of daylight. Perovskite solar cell has thermochromic properties which also make it an efficient  
628 switchable FIPV technology. This change occurs because of the influence of temperature and humidity.  
629 In the presence of moisture, and exposure time, Perovskite gets hydrated (either mono or di) but is  
630 capable to regain its original structure upon releasing the water molecules (Halder et al., 2015).

631 Inorganic  $\text{CsPbI}_{3-x}\text{Br}_x$  perovskite window changed its visible transparency between 81.7% transparent  
632 cold state to a 35.4% coloured hot state and also maintained 7% device efficiency in the coloured hot  
633 state. However, this material offered stability even after switching cycles. However, their transition  
634 temperature (100–350 °C) and switching time (up to 25 h) are significantly high for consideration as a  
635 window application. In general,  $\text{CsPbI}_3$  has a transition temperature close to 200°C which was reduced  
636 to 100°C by the inclusion of Br (Lin et al., 2018). In another work (as shown in **Figure 11a**), at room  
637 temperature, 91% transparent Perovskite in the visible range had the transition temperature at 43 °C  
638 while the relative humidity was less than 60%. Perovskite transition time was less than 5 min. This  
639 window was able to reduce the 2.5°C indoor temperature compared to traditional windows while  
640 characterised by external ambient direct sunlight in Hong Kong (Zhang et al., 2019). In another work,  
641 thermochromic perovskite (methylammonium lead iodide-methylamine complex  
642  $(\text{CH}_3\text{NH}_3\text{PbI}_3 \cdot x\text{CH}_3\text{NH}_2)$ ) changed its transmission between 68% visible in the bleached state to 3%  
643 visible transmittance in coloured state and conversion efficiencies was 11.3% in the colored state. Over  
644 20 switching cycle was achieved from this device (Wheeler et al., 2017). Liquid biconstituent  
645  $\text{MAPbBr}_{3-x}\text{I}_x$  perovskite solution became yellow, orange, red and dark red due to the heat treatment at  
646 25°C, 60°C, 90°C and 120°C respectively. The required time to reach from 25°C to 120°C was  
647 inversely proportional to the temperature (De Bastiani et al., 2017). This colour change process was  
648 stable and reversible. Recently, nanorods based  $\text{CH}_3\text{NH}_3\text{PbIBr}_2$  showed high transparency of ~92% at  
649 22 °C and 30% at 60 °C. This semi-switchable FIPV one changed its colour yellow at 22 °C to reddish-  
650 brown at 40 °C and at (60 °C) became maroon (**shown in Figure 11 b**) (Roy et al., 2021).

651 Another way to change the transmission for FIPV is possible by including switchable material with  
652 FIPV. The electrically activated smart switchable window is popular for adaptive less energy-hungry  
653 building integration. Currently, electrochromic (EC)(Bui et al., 2021), suspended particle device  
654 (SPD)(Ghosh and Norton, 2017b) and polymer dispersed liquid crystal (PDLC)(Ghosh and Mallick,  
655 2018a, 2018b) are the popular three electrically activated smart windows. Combining EC and PV is  
656 called photoelectrochromic or photovoltachromic (Cannavale et al., 2016). Silicon solar cell-based PV  
657 was reported which suffers from low optical contrast between transparent and opaque states (Deb et al.,  
658 2001). Later DSSC(Costa et al., 2019) and solution type EC (Huang et al., 2012) based switchable  
659 system was also developed. Further Perovskite solar cell-based EC window was also investigated for  
660 switchable PV application (Cannavale et al., 2015). Ghosh et.al. investigated an outdoor experiment at  
661 Dublin climatic condition where SPD was switched by powering silicon-based PV module and observed  
662 tremendous potential in this sector (Ghosh et al., 2016b). Polymer dispersed liquid crystal has the  
663 potential to improve the building interior by providing complete privacy when no power is applied and  
664 transmission when power is applied(Ghosh et al., 2018a). This PDLC film can be integrated with first  
665 and second-generation PV. If the PDLC film is placed on the top of the solar cell it can also control the

666 light intensity on the cell. On the other hand, if the PDLC film is placed in the backside of the PV then  
 667 PV can get uninterrupted light while depending on the occupant’s criteria transmission and opaque state  
 668 from the combined system is achievable (Khalid et al., 2021).

669



670

671 Figure 11: (a) Schematics of the cold to hot state transition by heating (dehydration) and the hot to  
 672 cold state by cooling (hydration)(Zhang et al., 2019) (b) Photographs of Semi-switching properties of  
 673 MAPbI<sub>3</sub> based perovskite FIPV(Roy et al., 2021).

674

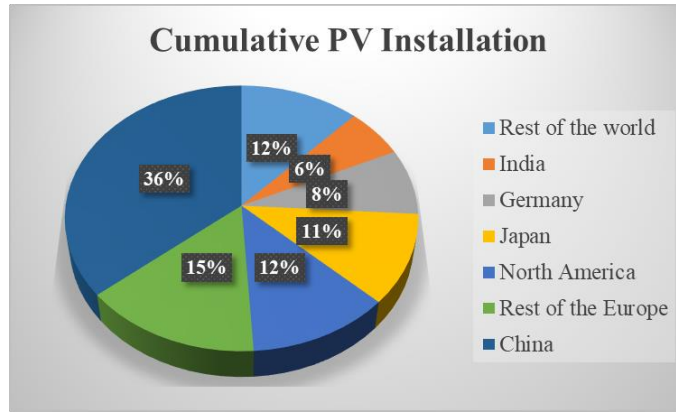
675

## 676 5. Discussion and perspective

677

### 678 5.1. Cost of FIPV

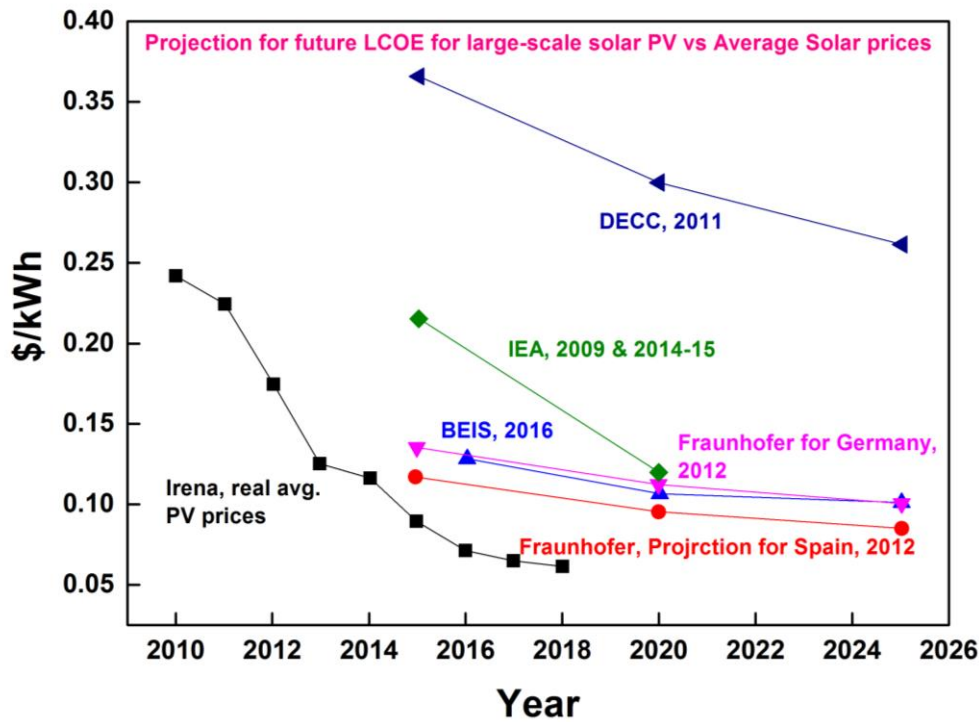
679 Installed photovoltaic (PV) capacity exceeded 500 GW at the end of 2018, and by 2023 an additional  
 680 500 GW of PV capacity is projected to be installed which will bring us into the era of TW-scale PV  
 681 (Haegel et al., 2019). Thus, a 600-fold enhancement of global photovoltaic capacity has been  
 682 experienced in the past two decades. **Figure 12** depicts the current cumulative PV installation globally.  
 683 The key driver to boost this market growth is the 99% cost reduction of crystalline Si (c-Si) PV cells  
 684 since 1980. It is estimated that the efficiency improvement has 23% contribution to this global  
 685 expansion while private and public R&D contributed an estimated 22% and 59% respectively for the  
 686 PV cost reduction between 1980 and 2012 (Kavлак et al., 2018). Solar energy system’s cost includes  
 687 soft cost because of the supply chain, installation for labour, relevant permits, overhead costs such as  
 688 marketing and hardware cost or equipment costs which is due to a module, inverter and electric wiring  
 689 cost, cost of a tracking system. Reduction of soft cost is currently under consideration as this sometimes  
 690 accounts for 80% of the PV system installation cost. Price can be further decreased because of  
 691 knowledge of spillover (“Knowledge spillovers occur when firms do not capture all the benefits from  
 692 investments in innovation because a portion of the knowledge created “spills over” to other firms”)  
 693 (Nemet et al., 2020). Over the past decade, levelized cost of electricity (LCOE) for solar PVs are  
 694 forecasted as shown in **Figure 13**. It is evident that all optimistic outlooks are actually wrong and within  
 695 a few years, all initial projections are now outdated. The price for FIPV is still not available very  
 696 straightforward like other single or double glazing windows. If BIPV is considered as whole building  
 697 skin, for all European regions, the northern façade is suitable considering all societal and environmental  
 698 benefits. BIPV building skin can always reimburse the investment cost and building can work as a  
 699 source of income (Gholami and Røstvik, 2020).



700

701 Figure 12: The total cumulative installations amounted to 584 GWp at the end of the year 2019  
 702 (Systems, 2021)

703



704

705 Figure 13: Forecasts for the levelized cost of electricity (LCOE) of solar PV (Tasgas, 2021)

706

707

708 **5.2. Technical reliability**

709 As PV solar power plant needs a considerable amount of land, integration of PV into the roof was  
 710 adopted. However, the limited rooftop area in most of the high rise buildings in urban locations cannot  
 711 offset the energy demands supplied by PV. Thus, BIPV and particularly BIPV window (FIPV) can be  
 712 a potential option as it not only generates power but also offers privacy and solar heat gain reduction  
 713 and heat loss reduction. Currently, European Nearly Zero Energy Building requires on-site renewable  
 714 energy production which is possible by employing more BIPV windows or FIPV integration. However,  
 715 in an urban location, an urban heat island is now a major issue that increases the urban ambient and also  
 716 the surface temperature of the building. This enhanced air temperature can also increase the PV cell

717 temperature can degrade the performance. However, the employment of thin-film or 3<sup>rd</sup> generation  
 718 based FIPV can eliminate the challenges because of their weak relation between temperature and  
 719 efficiency compared to first-generation silicon. Also, due to the dense and compact placing of building  
 720 in an urban location, shading is predominant which also reduce the power generation (Boccalatte et al.,  
 721 2020). As FIPV is not the best-oriented surface, and also solar radiation impinges on the vertical surface  
 722 is lower than horizontal surface thus further lower power generation is expected from any generation  
 723 PV based FIPV compared to their rated values. However, if we consider the recent trend of glassy  
 724 commercial buildings where façades possess larger areas compared to the roof then FIPV has great  
 725 potential. In addition, vertical FIPV facades receive more solar radiation in winter and early and late  
 726 hours of any day (when sun position is lower in the sky) which can produce relatively higher power  
 727 than summer and mid-day period. It is well established that the solar radiation reaching a surface is the  
 728 inclusion of direct, diffuse and reflected components. Bi-facial solar cell technology should come more  
 729 on the front as it can work with diffuse and reflection components from both ends. Commercialization  
 730 of an integrated FIPV is challenging because of the lack of available information which is available for  
 731 traditional PV systems which are either rack-mounted or ground-mounted.

732

733 **5.3. Perspective**

734 Hence, a smooth entry of the BIPV window or FIPV, collaborative links between different stakeholders  
 735 are essential. Initiatives from government and then BIPV industry and building construction and  
 736 architectural people conjunction with academia can enhance the installation for new and retrofit  
 737 buildings. Building users understanding and motivations are also key for any new technological  
 738 integration. While other advanced windows can work as retrofitted, BIPV needs special arrangements  
 739 because of the presence of electrical connections. A clear standard must be introduced which can be  
 740 country-specific or based on Kopean climate-specific. However, currently, most of the BIPV reports on  
 741 power generation, heat loss and gain properties, semitransparency level. Noise protection and fire  
 742 protection (Cancelliere et al., 2021) ability by BIPV is not a very popular research interest; nevertheless,  
 743 they are also the most prominent sector where more exploration must be prepared. If BIPV windows  
 744 are treated with replacement of traditional windows then snow (Borrebaek et al., 2020) and dust (Ghosh,  
 745 2020b) accumulation must not be ignored. While for traditional windows, dust or snow-covered can  
 746 just create issues with visual impact and daylight, for BIPV it can stop the power generation or will  
 747 generate power at much lower rates. Depending on the local climate, the cleaning mechanism should  
 748 be prearranged. Self-cleaning methods can predominate the BIPV window industry in future (Nundy et  
 749 al., 2021a, 2020). **Table 2** documented the difference between traditional (single and double glazed)  
 750 window and BIPV window

751 Table 2: Comparative analysis between a traditional window and BIPV window (FIPV)

Property	Traditional window	BIPV window
Purpose	Visual impact and connection between interior to exterior	Visual impact and power generation
Transparency	Single glazing~90% Double glazing~80%	Depends on the type of PV cell
Cost	Well advanced technology and depends on the supplier cost is decided. Recently ISSOL , Belgium based solar glass manufacturer estimated the cost for air-filled double glazing 200 euro/m <sup>2</sup>	Cost depends on the global market PV price and due to immature technology no standard rate is available. ISSOL estimated the price for silicon based BIPV window 350 euro/m <sup>2</sup>

Protection (noise and fire) ability	Traditional single and double glazing are not efficient. There are specific types available to perform this.	Few investigations have been done to know the capability to tackle these challenges.
Hot Climate application	Single glazing is better as they have a high $U$ -value, however high transmission allows excess heat and light	Very potential as it stops the solar energy penetration (including daylight)
Cold Climate application	Double glazing performs better than single glazing due to its low $U$ -value. Triple or multiple pane windows performs well. No control over daylight and heat.	Modification is required. Vacuum integrated BIPV can be a suitable option as they possess significant low $U$ -values

752

753

## 754 6. Conclusions

755 In this work, three different generations of solar PV system for building integrated photovoltaic (BIPV)  
756 window or fenestration integration PV (FIPV) was employed. For windows applications, PV must be  
757 transparent or semi-transparent type. Thus, first-generation PV which is opaque in nature must be  
758 spaced types whereas second generation and third generation are suitable. One of the main challenges  
759 for the wide adoption of BIPV windows is the optimisation of both daylighting and electricity  
760 generation. In this work, the key conclusions are

- 761 • c-Si-based spaced type BIPV is still under consideration and ready to install stage because of
- 762 the maturity, however, 2<sup>nd</sup> and third-generation PV based FIPV should be commanding in future
- 763 • advanced FIPV technologies can control the four essential factors ( $U$ -value, SHGC, CCT, CRI)
- 764 required for window application
- 765 • switchable FIPV can be a great alternative compared to static FIPV as it will behave with
- 766 occupants demand and generate benign power
- 767 • bi facial PV based FIPV has more ability to generate power than any other technology and can
- 768 be a great alternative for future FIPV
- 769 • Currently, most of the FIPV only consider transmission and power generation however
- 770 inclusion for the window frame and how they behave as a combined system will be an
- 771 interesting approach.

772

773

## 774 Reference

775

776 Aburas, M., Soebarto, V., Williamson, T., Liang, R., Ebendorff-Heidepriem, H., Wu, Y., 2019.  
777 Thermochromic smart window technologies for building application: A review. Appl. Energy  
778 255, 113522. <https://doi.org/10.1016/j.apenergy.2019.113522>

779 Alrashidi, H., Ghosh, A., Issa, W., Sellami, N., Mallick, T.K., Sundaram, S., 2020a. Thermal  
780 performance of semitransparent CdTe BIPV window at temperate climate. Sol. Energy 195,  
781 536–543. <https://doi.org/10.1016/j.solener.2019.11.084>

782 Alrashidi, H., Ghosh, A., Issa, W., Sellami, N., Mallick, T.K., Sundaram, S., 2019. Evaluation of solar  
783 factor using spectral analysis for CdTe photovoltaic glazing. Mater. Lett. 237, 332–335.

- 784 <https://doi.org/10.1016/j.matlet.2018.11.128>
- 785 Alrashidi, H., Issa, W., Sellami, N., Ghosh, A., Mallick, T.K., Sundaram, S., 2020b. Performance  
786 assessment of cadmium telluride-based semi-transparent glazing for power saving in façade  
787 buildings. *Energy Build.* 215, 109585. <https://doi.org/10.1016/j.enbuild.2019.109585>
- 788 Asghar, M.I., Zhang, J., Wang, H., Lund, P.D., 2017. Device stability of perovskite solar cells – A  
789 review. *Renew. Sustain. Energy Rev.* 77, 131–146. <https://doi.org/10.1016/j.rser.2017.04.003>
- 790 Aste, N., Buzzetti, M., Del Pero, C., Fusco, R., Testa, D., Leonforte, F., 2017. Visual Performance of  
791 Yellow, Orange and Red LSCs Integrated in a Smart Window. *Energy Procedia* 105, 967–972.  
792 <https://doi.org/10.1016/j.egypro.2017.03.427>
- 793 Baig, H., Kanda, H., Asiri, A.M., Nazeeruddin, M.K., Mallick, T., 2020. Increasing efficiency of  
794 perovskite solar cells using low concentrating photovoltaic systems. *Sustain. Energy Fuels.*  
795 <https://doi.org/10.1039/C9SE00550A>
- 796 Ballif, C., Perret-Aebi, L.E., Lufkin, S., Rey, E., 2018. Integrated thinking for photovoltaics in  
797 buildings. *Nat. Energy* 3, 438–442. <https://doi.org/10.1038/s41560-018-0176-2>
- 798 Barman, S., Chowdhury, A., Mathur, S., Mathur, J., 2018. Assessment of the efficiency of window  
799 integrated CdTe based semi-transparent photovoltaic module. *Sustain. Cities Soc.* 37, 250–262.  
800 <https://doi.org/10.1016/j.scs.2017.09.036>
- 801 Bellini, E., 2021. First Solar claims lowest module degradation rate in the industry. *PV Mag.*  
802 [https://doi.org/https://www.pv-magazine.com/2021/04/19/first-solar-claims-lowest-module-](https://doi.org/https://www.pv-magazine.com/2021/04/19/first-solar-claims-lowest-module-degradation-rate-in-the-industry/)  
803 [degradation-rate-in-the-industry/](https://doi.org/https://www.pv-magazine.com/2021/04/19/first-solar-claims-lowest-module-degradation-rate-in-the-industry/)
- 804 Bhandari, S., Ghosh, A., Roy, A., Mallick, T.K., Sundaram, S., 2022. Compelling Temperature  
805 Behaviour of Carbon-perovskite Solar Cell for Fenestration at Various Climates. *Chem. Eng. J.*  
806 *Adv.* 100267. <https://doi.org/10.1016/j.cej.2022.100267>
- 807 Bhandari, S., Roy, A., Ghosh, A., Mallick, T.K., Sundaram, S., 2020. Perceiving the temperature  
808 coefficients of carbon-based perovskite solar cells. *Sustain. Energy Fuels* 4, 6283–6298.  
809 <https://doi.org/10.1039/d0se00782j>
- 810 Boccalatte, A., Fossa, M., Ménézo, C., 2020. Best arrangement of BIPV surfaces for future NZEB  
811 districts while considering urban heat island effects and the reduction of reflected radiation from  
812 solar façades. *Renew. Energy* 160, 686–697. <https://doi.org/10.1016/j.renene.2020.07.057>
- 813 Borrebæk, P.O.A., Jelle, B.P., Zhang, Z., 2020. Avoiding snow and ice accretion on building  
814 integrated photovoltaics – challenges, strategies, and opportunities. *Sol. Energy Mater. Sol.*  
815 *Cells* 206. <https://doi.org/10.1016/j.solmat.2019.110306>
- 816 Bouvard, O., Vanzo, S., Schüler, A., 2015. Experimental determination of optical and thermal  
817 properties of semi-transparent photovoltaic modules based on dye-sensitized solar cells. *Energy*  
818 *Procedia* 78, 453–458. <https://doi.org/10.1016/j.egypro.2015.11.696>
- 819 Bristow, N., Kettle, J., 2018. Outdoor organic photovoltaic module characteristics: Benchmarking  
820 against other PV technologies for performance, calculation of Ross coefficient and outdoor  
821 stability monitoring. *Sol. Energy Mater. Sol. Cells* 175, 52–59.  
822 <https://doi.org/10.1016/j.solmat.2017.10.008>
- 823 Bui, D., Nguyen, T.N., Ghazlan, A., Ngo, T.D., 2021. Biomimetic adaptive electrochromic windows  
824 for enhancing building energy efficiency. *Appl. Energy* 300, 117341.  
825 <https://doi.org/10.1016/j.apenergy.2021.117341>
- 826 Buratti, C., Belloni, E., Merli, F., Zinzi, M., 2021. Aerogel glazing systems for building applications:  
827 A review. *Energy Build.* 231, 110587. <https://doi.org/10.1016/j.enbuild.2020.110587>
- 828 Büttner, B., Nauschütz, J., Heinemann, U., Reichenauer, G., Scherdel, C., Weinläder, H., Weismann,



- 829 S., Buck, D., Beck, A., 2019. Evacuated Glazing with Silica Aerogel Spacers, in: International  
830 Solar Energy Society; Euro Sun. pp. 1–8. <https://doi.org/10.18086/eurosun2018.06.17>
- 831 Cai, M., Wu, Y., Chen, H., Yang, X., Qiang, Y., Han, L., 2017. Cost-Performance Analysis of  
832 Perovskite Solar Modules. *Adv. Sci.* 4. <https://doi.org/10.1002/advs.201600269>
- 833 Cancelliere, P., Manzini, G., Traina, G., Gabriele, M., 2021. PV modules on buildings – Outlines of  
834 PV roof samples fire rating assessment. *Fire Saf. J.* 120, 103139.  
835 <https://doi.org/10.1016/j.firesaf.2020.103139>
- 836 Cannavale, A., Cossari, P., Eperon, G.E., Colella, S., Fiorito, F., Gigli, G., Snaith, H.J., Listorti, A.,  
837 2016. Forthcoming perspectives of photoelectrochromic devices: A critical review. *Energy*  
838 *Environ. Sci.* 9, 2682–2719. <https://doi.org/10.1039/c6ee01514j>
- 839 Cannavale, A., Eperon, G.E., Cossari, P., Abate, A., Snaith, H.J., Gigli, G., 2015. Perovskite  
840 photovoltaic cells for building integration. *Energy Environ. Sci.* 8, 1578–1584.  
841 <https://doi.org/10.1039/C5EE00896D>
- 842 Cannavale, A., H??rantner, M., Eperon, G.E., Snaith, H.J., Fiorito, F., Ayr, U., Martellotta, F., 2017.  
843 Building integration of semitransparent perovskite-based solar cells: Energy performance and  
844 visual comfort assessment. *Appl. Energy* 194, 94–107.  
845 <https://doi.org/10.1016/j.apenergy.2017.03.011>
- 846 Cerne, B., Kralj, A., Drev, M., Žnidarši, M., Hafner, J., Petter, B., 2019. Investigations of 6-pane  
847 glazing : Properties and possibilities. *Energy Build.* 190, 61–68.  
848 <https://doi.org/10.1016/j.enbuild.2019.02.033>
- 849 Chae, Y.T., Kim, J., Park, H., Shin, B., 2014. Building energy performance evaluation of building  
850 integrated photovoltaic (BIPV) window with semi-transparent solar cells. *Appl. Energy* 129,  
851 217–227. <https://doi.org/10.1016/j.apenergy.2014.04.106>
- 852 Chandrika, V.S., Thalib, M.M., Karthick, A., Sathyamurthy, R., Manokar, A.M., Subramaniam, U.,  
853 Stalin, B., 2021. Performance assessment of free standing and building integrated grid connected  
854 photovoltaic system for southern part of India. *Build. Serv. Eng. Res. Technol.* 42, 237–248.  
855 <https://doi.org/10.1177/0143624420977749>
- 856 Chen, B., Lv, H., Liao, J., Dong, S., Cheng, C., Lv, Q., Li, J., Su, Y., Riffat, S., 2019. Thermal  
857 insulation performance of an advanced photovoltaic vacuum glazing: A numerical investigation  
858 and simulation. *J. Renew. Sustain. Energy* 11. <https://doi.org/10.1063/1.5055363>
- 859 Chen, M., Ju, M.G., Garces, H.F., Carl, A.D., Ono, L.K., Hawash, Z., Zhang, Y., Shen, T., Qi, Y.,  
860 Grimm, R.L., Pacifici, D., Zeng, X.C., Zhou, Y., Padture, N.P., 2019. Highly stable and efficient  
861 all-inorganic lead-free perovskite solar cells with native-oxide passivation. *Nat. Commun.* 10, 1–  
862 8. <https://doi.org/10.1038/s41467-018-07951-y>
- 863 Chen, M., Zhang, W., Xie, L., He, B., Wang, W., Li, J., Li, Z., 2021. Improvement of the electricity  
864 performance of bifacial PV module applied on the building envelope. *Energy Build.* 238,  
865 110849. <https://doi.org/10.1016/j.enbuild.2021.110849>
- 866 Choul, J., Sun, J., Chandrasekaran, N., Dunn, C.J., Anthony, S., Chesman, R., Jasieniak, J.J., 2020.  
867 Nano Energy Semi-transparent perovskite solar cells with a cross-linked hole transport layer.  
868 *Nano Energy* 71, 104635. <https://doi.org/10.1016/j.nanoen.2020.104635>
- 869 Chow, T.T., Fong, K.F., He, W., Lin, Z., Chan, A.L.S., 2007. Performance evaluation of a PV  
870 ventilated window applying to office building of Hong Kong. *Energy Build.* 39, 643–650.  
871 <https://doi.org/10.1016/j.enbuild.2006.09.014>
- 872 Chow, T.T., Lin, Z., He, W., Chan, A.L.S., Fong, K.F., 2006. Use of ventilated solar screen window  
873 in warm climate. *Appl. Therm. Eng.* 26, 1910–1918.  
874 <https://doi.org/10.1016/j.applthermaleng.2006.01.026>

- 875 Chow, T.T., Pei, G., Chan, L.S., Lin, Z., Fong, K.F., 2009. A comparative study of PV glazing  
876 performance in warm climate. *Indoor Built Environ.* 18, 32–40.  
877 <https://doi.org/10.1177/1420326X08100323>
- 878 Collins, R.E., Robinson, S.J., 1991. Evacuated glazing. *Sol. Energy* 47, 27–38.  
879 [https://doi.org/10.1016/0038-092X\(91\)90060-A](https://doi.org/10.1016/0038-092X(91)90060-A)
- 880 Collins, R.E., Turner, G.M., Fischer-Cripps, A.C., Tang, J.Z., Simko, T.M., Dey, C.J., Clugston,  
881 D.A., Zhang, Q.C., Garrison, J.D., 1995. Vacuum glazing-A new component for insulating  
882 windows. *Build. Environ.* 30, 459–492. [https://doi.org/10.1016/0360-1323\(95\)00025-2](https://doi.org/10.1016/0360-1323(95)00025-2)
- 883 Costa, C., Ivanou, D., Pinto, J., Mendes, J., Mendes, A., 2019. Impact of the architecture of dye  
884 sensitized solar cell-powered electrochromic devices on their photovoltaic performance and the  
885 ability to color change. *Sol. Energy* 182, 22–28. <https://doi.org/10.1016/j.solener.2019.02.036>
- 886 Cuce, E., Riffat, S.B., Young, C.H., 2015. Thermal insulation, power generation, lighting and energy  
887 saving performance of heat insulation solar glass as a curtain wall application in Taiwan: A  
888 comparative experimental study. *Energy Convers. Manag.* 96, 31–38.  
889 <https://doi.org/10.1016/j.enconman.2015.02.062>
- 890 De Bastiani, M., Saidaminov, M.I., Dursun, I., Sinatra, L., Peng, W., Buttner, U., Mohammed, O.F.,  
891 Bakr, O.M., 2017. Thermochromic Perovskite Inks for Reversible Smart Window Applications.  
892 *Chem. Mater.* 29, 3367–3370. <https://doi.org/10.1021/acs.chemmater.6b05112>
- 893 Deb, S.K., Lee, S.H., Edwin Tracy, C., Roland Pitts, J., Gregg, B.A., Branz, H.M., 2001. Stand-alone  
894 photovoltaic-powered electrochromic smart window. *Electrochim. Acta* 46, 2125–2130.  
895 [https://doi.org/10.1016/S0013-4686\(01\)00390-5](https://doi.org/10.1016/S0013-4686(01)00390-5)
- 896 Deceglie, M.G., Silverman, T.J., Marion, B., Kurtz, S.R., 2014. Metastable changes to the temperature  
897 coefficients of thin-film photovoltaic modules. 2014 IEEE 40th Photovolt. Spec. Conf. PVSC  
898 2014 15, 337–340. <https://doi.org/10.1109/PVSC.2014.6924926>
- 899 Deline, C., Macalpine, S., Olalla, C., 2020. Estimating and parameterizing mismatch power loss in  
900 bifacial photovoltaic systems. *Prog. Photovoltaics* 28, 1–13. <https://doi.org/10.1002/pip.3259>
- 901 Dupré, O., Vaillon, R., Green, M.A., 2015. Physics of the temperature coefficients of solar cells. *Sol.*  
902 *Energy Mater. Sol. Cells* 140, 92–100. <https://doi.org/10.1016/j.solmat.2015.03.025>
- 903 Eperon, G.E., Burlakov, V.M., Docampo, P., Goriely, A., Snaith, H.J., 2014a. Morphological control  
904 for high performance, solution-processed planar heterojunction perovskite solar cells. *Adv.*  
905 *Funct. Mater.* 24, 151–157. <https://doi.org/10.1002/adfm.201302090>
- 906 Eperon, G.E., Burlakov, V.M., Goriely, A., Snaith, H.J., 2014b. Neutral color semitransparent  
907 microstructured perovskite solar cells. *ACS Nano* 8, 591–598.  
908 <https://doi.org/10.1021/nn4052309>
- 909 Fang, Y., Hyde, T.J., Arya, F., Hewitt, N., Eames, P.C., Norton, B., Miller, S., 2014. Indium alloy-  
910 sealed vacuum glazing development and context. *Renew. Sustain. Energy Rev.* 37, 480–501.  
911 <https://doi.org/10.1016/j.rser.2014.05.029>
- 912 Feng, F., Kunwar, N., Cetin, K., Neill, Z.O., 2021. Energy & Buildings A critical review of  
913 fenestration / window system design methods for high performance buildings. *Energy Build.*  
914 248, 111184. <https://doi.org/10.1016/j.enbuild.2021.111184>
- 915 Feng, W., Zou, L., Gao, G., Wu, G., Shen, J., Li, W., 2016. Gasochromic smart window: Optical and  
916 thermal properties, energy simulation and feasibility analysis. *Sol. Energy Mater. Sol. Cells* 144,  
917 316–323. <https://doi.org/10.1016/j.solmat.2015.09.029>
- 918 Feng, Y., Duan, Q., Wang, J., Baur, S., 2020. Approximation of building window properties using in  
919 situ measurements. *Build. Environ.* 169, 106590. <https://doi.org/10.1016/j.buildenv.2019.106590>

- 920 Friman, M., Geoola, F., Yehia, I., Ozer, S., Levi, A., Magadley, E., Brikman, R., Rosenfeld, L., Levy,  
921 A., Kacira, M., Teitel, M., 2019. Testing organic photovoltaic modules for application as  
922 greenhouse cover or shading element. *Biosyst. Eng.* 184, 24–36.  
923 <https://doi.org/10.1016/j.biosystemseng.2019.05.003>
- 924 Fu, R., James, T.L., Woodhouse, M., 2015. Economic measurements of polysilicon for the  
925 photovoltaic industry: Market competition and manufacturing competitiveness. *IEEE J.*  
926 *Photovoltaics* 5, 515–524. <https://doi.org/10.1109/JPHOTOV.2014.2388076>
- 927 Gevorgyan, S.A., Madsen, M. V, Dam, H.F., Jørgensen, M., Fell, C.J., Anderson, K.F., Duck, B.C.,  
928 Mescheloff, A., Katz, E.A., Elschner, A., Roesch, R., Hoppe, H., Hermenau, M., Riede, M.,  
929 Krebs, F.C., 2013. Solar Energy Materials & Solar Cells Interlaboratory outdoor stability studies  
930 of flexible roll-to-roll coated organic photovoltaic modules : Stability over 10 , 000 h. *Sol.*  
931 *Energy Mater. Sol. Cells* 116, 187–196. <https://doi.org/10.1016/j.solmat.2013.04.024>
- 932 Gholami, H., Røstvik, H.N., 2020. Economic analysis of BIPV systems as a building envelope  
933 material for building skins in Europe. *Energy* 204, 117931.  
934 <https://doi.org/10.1016/j.energy.2020.117931>
- 935 Ghosh, A., 2020a. Potential of building integrated and attached/applied photovoltaic (BIPV/BAPV)  
936 for adaptive less energy-hungry building's skin: A comprehensive Review. *J. Clean. Prod.*  
937 123343. <https://doi.org/10.1016/j.jclepro.2020.123343>
- 938 Ghosh, A., 2020b. Soiling Losses : A Barrier for India ' s Energy Security Dependency from  
939 Photovoltaic Power. *Challenges* 11, 1–9. <https://doi.org/10.3390/challe11010009>
- 940 Ghosh, A., Bhandari, S., Sundaram, S., Mallick, T.K., 2020. Carbon counter electrode mesoscopic  
941 ambient processed & characterised perovskite for adaptive BIPV fenestration. *Renew.*  
942 *Energy* 145, 2151–2158. <https://doi.org/10.1016/j.renene.2019.07.119>
- 943 Ghosh, A., Mallick, T.K., 2018a. Evaluation of optical properties and protection factors of a PDLC  
944 switchable glazing for low energy building integration. *Sol. Energy Mater. Sol. Cells* 176, 391–  
945 396. <https://doi.org/10.1016/j.solmat.2017.10.026>
- 946 Ghosh, A., Mallick, T.K., 2018b. Evaluation of colour properties due to switching behaviour of a  
947 PDLC glazing for adaptive building integration. *Renew. Energy* 120, 126–133.  
948 <https://doi.org/10.1016/j.renene.2017.12.094>
- 949 Ghosh, A., Norton, B., 2019. Optimization of PV powered SPD switchable glazing to minimise  
950 probability of loss of power supply. *Renew. Energy* 131, 993–1001.  
951 <https://doi.org/10.1016/j.renene.2018.07.115>
- 952 Ghosh, A., Norton, B., 2018. Advances in switchable and highly insulating autonomous (self-  
953 powered) glazing systems for adaptive low energy buildings. *Renew. Energy* 126, 1003–1031.  
954 <https://doi.org/10.1016/j.renene.2018.04.038>
- 955 Ghosh, A., Norton, B., 2017a. Interior colour rendering of daylight transmitted through a suspended  
956 particle device switchable glazing. *Sol. Energy Mater. Sol. Cells* 163, 218–223.  
957 <https://doi.org/10.1016/j.solmat.2017.01.041>
- 958 Ghosh, A., Norton, B., 2017b. Durability of switching behaviour after outdoor exposure for a  
959 suspended particle device switchable glazing. *Sol. Energy Mater. Sol. Cells* 163, 178–184.  
960 <https://doi.org/10.1016/j.solmat.2017.01.036>
- 961 Ghosh, A., Norton, B., Duffy, A., 2017. Effect of sky clearness index on transmission of evacuated  
962 (vacuum) glazing. *Renew. Energy* 105, 160–166. <https://doi.org/10.1016/j.renene.2016.12.056>
- 963 Ghosh, A., Norton, B., Duffy, A., 2016a. Measured thermal & daylight performance of an evacuated  
964 glazing using an outdoor test cell. *Appl. Energy* 177, 196–203.  
965 <https://doi.org/10.1016/j.apenergy.2016.05.118>

- 966 Ghosh, A., Norton, B., Duffy, A., 2016b. First outdoor characterisation of a PV powered suspended  
967 particle device switchable glazing. *Sol. Energy Mater. Sol. Cells* 157, 1–9.  
968 <https://doi.org/10.1016/j.solmat.2016.05.013>
- 969 Ghosh, A., Norton, B., Mallick, T.K., 2018a. Influence of atmospheric clearness on PDLC switchable  
970 glazing transmission. *Energy Build.* 172, 257–264. <https://doi.org/10.1016/j.enbuild.2018.05.008>
- 971 Ghosh, A., Sarmah, N., Sundaram, S., Mallick, T.K., 2019a. Numerical studies of thermal comfort for  
972 semi-transparent building integrated photovoltaic ( BIPV ) -vacuum glazing system. *Sol. Energy*  
973 190, 608–616. <https://doi.org/10.1016/j.solener.2019.08.049>
- 974 Ghosh, A., Selvaraj, P., Sundaram, S., Mallick, T.K., 2018b. The colour rendering index and  
975 correlated colour temperature of dye-sensitized solar cell for adaptive glazing application. *Sol.*  
976 *Energy* 163, 537–544. <https://doi.org/10.1016/j.solener.2018.02.021>
- 977 Ghosh, A., Sundaram, S., Mallick, T.K., 2019b. Colour properties and glazing factors evaluation of  
978 multicrystalline based semi-transparent Photovoltaic-vacuum glazing for BIPV application.  
979 *Renew. Energy* 131, 730–736. <https://doi.org/10.1016/j.renene.2018.07.088>
- 980 Ghosh, A., Sundaram, S., Mallick, T.K., 2018c. Investigation of thermal and electrical performances  
981 of a combined semi-transparent PV-vacuum glazing. *Appl. Energy* 228, 1591–1600.  
982 <https://doi.org/10.1016/j.apenergy.2018.07.040>
- 983 Gong, J., Liang, J., Sumathy, K., 2012. Review on dye-sensitized solar cells (DSSCs): Fundamental  
984 concepts and novel materials. *Renew. Sustain. Energy Rev.* 16, 5848–5860.  
985 <https://doi.org/10.1016/j.rser.2012.04.044>
- 986 Gorgolis, G., Karamanis, D., 2016. Solar energy materials for glazing technologies. *Sol. Energy*  
987 *Mater. Sol. Cells* 144, 559–578. <https://doi.org/10.1016/j.solmat.2015.09.040>
- 988 Green, M., Dunlop, E., Hohl-Ebinger, J., Yoshita, M., Kopidakis, N., Hao, X., 2020. Solar cell  
989 efficiency tables (version 57). *Prog. Photovoltaics Res. Appl.* 1–13.  
990 <https://doi.org/10.1002/pip.3371>
- 991 Green, M.A., 2005. Silicon photovoltaic modules: A brief history of the first 50 years. *Prog.*  
992 *Photovoltaics Res. Appl.* 13, 447–455. <https://doi.org/10.1002/pip.612>
- 993 Green, M.A., Hishikawa, Y., Dunlop, E.D., Levi, D.H., Hohl-Ebinger, J., Yoshita, M., Ho-Baillie,  
994 A.W.Y., 2019. Solar cell efficiency tables (Version 53). *Prog. Photovoltaics Res. Appl.* 27, 3–  
995 12. <https://doi.org/10.1002/pip.3102>
- 996 Greijer, H., Karlson, L., Lindquist, S.E., Hagfeldt, A., 2001. Environmental aspects of electricity  
997 generation from a nanocrystalline dye sensitized solar cell system. *Renew. energy* 23, 27–39.  
998 [https://doi.org/10.1016/S0960-1481\(00\)00111-7](https://doi.org/10.1016/S0960-1481(00)00111-7)
- 999 Griffiths, P.W., Di Leo, M., Cartwright, P., Eames, P.C., Yianoulis, P., Leftheriotis, G., Norton, B.,  
1000 1998. Fabrication of evacuated glazing at low temperature. *Sol. Energy* 63, 243–249.  
1001 [https://doi.org/10.1016/S0038-092X\(98\)00019-X](https://doi.org/10.1016/S0038-092X(98)00019-X)
- 1002 Gu, W., Ma, T., Li, M., Shen, L., Zhang, Y., 2020. A coupled optical-electrical-thermal model of the  
1003 bifacial photovoltaic module. *Appl. Energy* 258, 114075.  
1004 <https://doi.org/10.1016/j.apenergy.2019.114075>
- 1005 Guerrero-lemus, R., Vega, R., Kim, T., Kimm, A., Shephard, L.E., 2016. Bifacial solar photovoltaics  
1006 – A technology review. *Renew. Sustain. Energy Rev.* 60, 1533–1549.  
1007 <https://doi.org/10.1016/j.rser.2016.03.041>
- 1008 Haegel, N.M., Atwater, H., Barnes, T., Breyer, C., Burrell, A., Chiang, Y.-M., De Wolf, S., Dimmler,  
1009 B., Feldman, D., Glunz, S., Goldschmidt, J.C., Hochschild, D., Inzunza, R., Kaizuka, I.,  
1010 Kroposki, B., Kurtz, S., Leu, S., Margolis, R., Matsubara, K., Metz, A., Metzger, W.K.,

- 1011 Morjaria, M., Niki, S., Nowak, S., Peters, I.M., Philipps, S., Reindl, T., Richter, A., Rose, D.,  
 1012 Sakurai, K., Schlatmann, R., Shikano, M., Sinke, W., Sinton, R., Stanbery, B.J., Topic, M.,  
 1013 Tumas, W., Ueda, Y., van de Lagemaat, J., Verlinden, P., Vetter, M., Warren, E., Werner, M.,  
 1014 Yamaguchi, M., Bett, A.W., 2019. Terawatt-scale photovoltaics: Transform global energy.  
 1015 *Science* (80-. ). 364, 836–838. <https://doi.org/10.1126/science.aaw1845>
- 1016 Halder, A., Choudhury, D., Ghosh, S., Subbiah, A.S., Sarkar, S.K., 2015. Exploring Thermo-chromic  
 1017 Behavior of Hydrated Hybrid Perovskites in Solar Cells. *J. Phys. Chem. Lett.* 6, 3180–3184.  
 1018 <https://doi.org/10.1021/acs.jpcclett.5b01426>
- 1019 He, W., Zhang, Y.X., Sun, W., Hou, J.X., Jiang, Q.Y., Ji, J., 2011. Experimental and numerical  
 1020 investigation on the performance of amorphous silicon photovoltaics window in East China.  
 1021 *Build. Environ.* 46, 363–369. <https://doi.org/10.1016/j.buildenv.2010.07.030>
- 1022 Holzhey, P., Saliba, M., 2018. A full overview of international standards assessing the long-term  
 1023 stability of perovskite solar cells. *J. Mater. Chem. A* 6, 21794–21808.  
 1024 <https://doi.org/10.1039/C8TA06950F>
- 1025 Huang, J., Chen, X., Peng, J., Yang, H., 2021. Modelling analyses of the thermal property and heat  
 1026 transfer performance of a novel composite PV vacuum glazing. *Renew. Energy* 163, 1238–  
 1027 1252. <https://doi.org/10.1016/j.renene.2020.09.027>
- 1028 Huang, J., Chen, X., Yang, H., Zhang, W., 2018. Numerical investigation of a novel vacuum  
 1029 photovoltaic curtain wall and integrated optimization of photovoltaic envelope systems. *Appl.*  
 1030 *Energy* 229, 1048–1060. <https://doi.org/10.1016/j.apenergy.2018.08.095>
- 1031 Huang, L.M., Hu, C.W., Liu, H.C., Hsu, C.Y., Chen, C.H., Ho, K.C., 2012. Photovoltaic  
 1032 electrochromic device for solar cell module and self-powered smart glass applications. *Sol.*  
 1033 *Energy Mater. Sol. Cells* 99, 154–159. <https://doi.org/10.1016/j.solmat.2011.03.036>
- 1034 Iea-pvps, R., 2018. International definitions of BIPV.
- 1035 Jarimi, H., Lv, Q., Omar, R., Zhang, S., Riffat, S., 2020. Design, mathematical modelling and  
 1036 experimental investigation of vacuum insulated semi-transparent thin-film photovoltaic (PV)  
 1037 glazing. *J. Build. Eng.* 31, 101430. <https://doi.org/10.1016/j.jobe.2020.101430>
- 1038 Kabilan, R., Chandran, V., Yogapriya, J., Karthick, A., Gandhi, P.P., Mohanavel, V., Rahim, R.,  
 1039 Manoharan, S., 2021. Short-Term Power Prediction of Building Integrated Photovoltaic (BIPV)  
 1040 System Based on Machine Learning Algorithms. *Int. J. Photoenergy* 2021.  
 1041 <https://doi.org/10.1155/2021/5582418>
- 1042 Kaliappan, S., Saravanakumar, R., Karthick, A., Kumar, P.M., Venkatesh, V., Mohanavel, V.,  
 1043 Rajkumar, S., 2021. Hourly and Day Ahead Power Prediction of Building Integrated  
 1044 Semitransparent Photovoltaic System. *Int. J. Photoenergy* 2021.
- 1045 Kang, J.G., Kim, J.H., Kim, J.T., 2013. Performance evaluation of DSC windows for buildings. *Int. J.*  
 1046 *Photoenergy* 2013. <https://doi.org/10.1155/2013/472086>
- 1047 Kang, M.G., Park, N.G., Park, Y.J., Ryu, K.S., Chang, S.H., 2003. Manufacturing method for  
 1048 transparent electric windows using dye-sensitized TiO<sub>2</sub> solar cells. *Sol. Energy Mater. Sol. Cells*  
 1049 75, 475–479. [https://doi.org/10.1016/S0927-0248\(02\)00202-7](https://doi.org/10.1016/S0927-0248(02)00202-7)
- 1050 Karthick, A., Kalidasa Murugavel, K., Kalaivani, L., 2018a. Performance analysis of semitransparent  
 1051 photovoltaic module for skylights. *Energy* 162, 798–812.  
 1052 <https://doi.org/10.1016/j.energy.2018.08.043>
- 1053 Karthick, A., Kalidasa Murugavel, K., Kalaivani, L., Saravana Babu, U., 2018b. Performance study of  
 1054 building integrated photovoltaic modules. *Adv. Build. Energy Res.* 12, 178–194.  
 1055 <https://doi.org/10.1080/17512549.2016.1275982>

- 1056 Karthick, A., Kalidasa Murugavel, K., Sudalaiyandi, K., Muthu Manokar, A., 2020. Building  
 1057 integrated photovoltaic modules and the integration of phase change materials for equatorial  
 1058 applications. *Build. Serv. Eng. Res. Technol.* 41, 634–652.  
 1059 <https://doi.org/10.1177/0143624419883363>
- 1060 Karthick, A., Murugavel, K.K., Ramanan, P., 2018c. Performance enhancement of a building-  
 1061 integrated photovoltaic module using phase change material. *Energy* 142, 803–812.  
 1062 <https://doi.org/10.1016/j.energy.2017.10.090>
- 1063 Kavlak, G., McNerney, J., Trancik, J.E., 2018. Evaluating the causes of cost reduction in photovoltaic  
 1064 modules. *Energy Policy* 123, 700–710. <https://doi.org/10.1016/j.enpol.2018.08.015>
- 1065 Khalid, M., Shanks, K., Ghosh, A., Tahir, A., Sundaram, S., Mallick, T.K., 2021. Temperature  
 1066 regulation of concentrating photovoltaic window using argon gas and polymer dispersed liquid  
 1067 crystal films. *Renew. Energy* 164, 96–108. <https://doi.org/10.1016/j.renene.2020.09.069>
- 1068 Kim, C., Sang, M., Ko, J., Ko, M., Gu, M., Song, H., 2021. Inhomogeneous rear reflector induced  
 1069 hot-spot risk and power loss in building-integrated bifacial c-Si photovoltaic modules. *Renew.*  
 1070 *Energy* 163, 825–835. <https://doi.org/10.1016/j.renene.2020.09.020>
- 1071 Knoop, M., Stefani, O., Bueno, B., Matusiak, B., Hobday, R., Wirz-Justice, A., Martiny, K.,  
 1072 Kantermann, T., Aarts, M.P.J., Zemmouri, N., Appelt, S., Norton, B., 2020. Daylight: What  
 1073 makes the difference? *Light. Res. Technol.* 52, 423–442.  
 1074 <https://doi.org/10.1177/1477153519869758>
- 1075 Kong, H., Yu, Z., Zhang, J., Han, Y., Wu, L., Wang, H., Wang, J., 2020. Perspective of CIGS-BIPV  
 1076 s Product Competitiveness in China. *Int. J. Photoenergy* 2020, 1–10.
- 1077 Kuhn, T.E., Erban, C., Heinrich, M., Eisenlohr, J., Ensslen, F., Neuhaus, D.H., 2021. Review of  
 1078 technological design options for building integrated photovoltaics (BIPV). *Energy Build.* 231,  
 1079 110381. <https://doi.org/10.1016/j.enbuild.2020.110381>
- 1080 Kumar, N.M., Samykan, M., Karthick, A., 2021. Energy loss analysis of a large scale BIPV system  
 1081 for university buildings in tropical weather conditions: A partial and cumulative performance  
 1082 ratio approach. *Case Stud. Therm. Eng.* 25, 100916. <https://doi.org/10.1016/j.csite.2021.100916>
- 1083 Lamers, M.W.P.E., Özkalay, E., Gali, R.S.R., Janssen, G.J.M., Weeber, A.W., Romijn, I.G., 2018.  
 1084 Solar Energy Materials and Solar Cells Temperature effects of bifacial modules : Hotter or  
 1085 cooler ? *Sol. Energy Mater. Sol. Cells* 185, 192–197.  
 1086 <https://doi.org/10.1016/j.solmat.2018.05.033>
- 1087 Lee, H.M., Yoon, J.H., 2018. Power performance analysis of a transparent DSSC BIPV window based  
 1088 on 2 year measurement data in a full-scale mock-up. *Appl. Energy* 225, 1013–1021.  
 1089 <https://doi.org/10.1016/j.apenergy.2018.04.086>
- 1090 Lee, J.W., Park, J., Jung, H.J., 2014. A feasibility study on a building's window system based on dye-  
 1091 sensitized solar cells. *Energy Build.* 81, 38–47. <https://doi.org/10.1016/j.enbuild.2014.06.010>
- 1092 Lee, T.D., Ebong, A.U., 2017. A review of thin film solar cell technologies and challenges. *Renew.*  
 1093 *Sustain. Energy Rev.* 70, 1286–1297. <https://doi.org/10.1016/j.rser.2016.12.028>
- 1094 Leite Didoné, E., Wagner, A., 2013. Semi-transparent PV windows: A study for office buildings in  
 1095 Brazil. *Energy Build.* 67, 136–142. <https://doi.org/10.1016/j.enbuild.2013.08.002>
- 1096 Li, G., Xuan, Q., Akram, M.W., Golizadeh Akhlaghi, Y., Liu, H., Shittu, S., 2020. Building integrated  
 1097 solar concentrating systems: A review. *Appl. Energy* 260, 114288.  
 1098 <https://doi.org/10.1016/j.apenergy.2019.114288>
- 1099 Liao, W., Xu, S., 2015. Energy performance comparison among see-through amorphous-silicon PV  
 1100 (photovoltaic) glazings and traditional glazings under different architectural conditions in China.

- 1101 Energy 83, 267–275. <https://doi.org/10.1016/j.energy.2015.02.023>
- 1102 Lin, J., Lai, M., Dou, L., Kley, C.S., Chen, H., Peng, F., Sun, J., Lu, D., Hawks, S.A., Xie, C., Cui, F.,  
1103 Alivisatos, A.P., Limmer, D.T., Yang, P., 2018. Thermochromic halide perovskite solar cells.  
1104 Nat. Mater. 17, 261–267. <https://doi.org/10.1038/s41563-017-0006-0>
- 1105 Liu, X., Wu, Y., 2021. Design, development and characterisation of a Building Integrated  
1106 Concentrating Photovoltaic (BICPV) smart window system. Sol. Energy 220, 722–734.  
1107 <https://doi.org/10.1016/j.solener.2021.03.037>
- 1108 Lorenzo, E., 2021. On the historical origins of bifacial PV modelling. Sol. Energy 218, 587–595.  
1109 <https://doi.org/10.1016/j.solener.2021.03.006>
- 1110 Lucera, L., Machui, F., Schmidt, H.D., Ahmad, T., Kubis, P., Strohm, S., Hepp, J., Vetter, A.,  
1111 Egelhaaf, H.J., Brabec, C.J., 2017. Printed semi-transparent large area organic photovoltaic  
1112 modules with power conversion efficiencies of close to 5 %. Org. Electron. physics, Mater.  
1113 Appl. 45, 209–214. <https://doi.org/10.1016/j.orgel.2017.03.013>
- 1114 Luo, W., Khoo, Y.S., Kumar, A., Low, J.S.C., Li, Y., Tan, Y.S., Wang, Y., Aberle, A.G.,  
1115 Ramakrishna, S., 2018. A comparative life-cycle assessment of photovoltaic electricity  
1116 generation in Singapore by multicrystalline silicon technologies. Sol. Energy Mater. Sol. Cells  
1117 174, 157–162. <https://doi.org/10.1016/j.solmat.2017.08.040>
- 1118 Memon, S., Fang, Y., Eames, P.C., 2019. The influence of low-temperature surface induction on  
1119 evacuation, pump-out hole sealing and thermal performance of composite edge-sealed vacuum  
1120 insulated glazing. Renew. Energy 135, 450–464. <https://doi.org/10.1016/j.renene.2018.12.025>
- 1121 Memon, S., Farukh, F., Eames, P.C., Silberschmidt, V. V., 2015. A new low-temperature hermetic  
1122 composite edge seal for the fabrication of triple vacuum glazing. Vacuum 120, 73–82.  
1123 <https://doi.org/10.1016/j.vacuum.2015.06.024>
- 1124 Meng, W., Jinqing, P., Hongxing, Y., Yimo, L., 2018. Performance evaluation of semi-transparent  
1125 CdTe thin film PV window applying on commercial buildings in Hong Kong. Energy Procedia  
1126 152, 1091–1096. <https://doi.org/10.1016/j.egypro.2018.09.131>
- 1127 Miyazaki, T., Akisawa, A., Kashiwagi, T., 2005. Energy savings of office buildings by the use of  
1128 semi-transparent solar cells for windows. Renew. Energy 30, 281–304.  
1129 <https://doi.org/10.1016/j.renene.2004.05.010>
- 1130 Morini, M., Corrao, R., 2017. Energy Optimization of BIPV Glass Blocks: A Multi-software Study.  
1131 Energy Procedia 111, 982–992. <https://doi.org/10.1016/j.egypro.2017.03.261>
- 1132 Mufti, N., Amrillah, T., Taufiq, A., 2020. Review of CIGS-based solar cells manufacturing by  
1133 structural engineering. Sol. Energy 207, 1146–1157.  
1134 <https://doi.org/10.1016/j.solener.2020.07.065>
- 1135 Mustafa, N.I., Ludin, N.A., Mohamed, N.M., Ibrahim, M.A., Teridi, M.A.M., Sepeai, S., Zaharim, A.,  
1136 Sopian, K., 2019. Environmental performance of window-integrated systems using dye-  
1137 sensitised solar module technology in Malaysia. Sol. Energy 187, 379–392.  
1138 <https://doi.org/10.1016/j.solener.2019.05.059>
- 1139 Nabil, A., Mardaljevic, J., 2006. Useful daylight illuminances: A replacement for daylight factors.  
1140 Energy Build. 38, 905–913. <https://doi.org/10.1016/j.enbuild.2006.03.013>
- 1141 Nemet, G.F., Lu, J., Rai, V., Rao, R., 2020. Knowledge spillovers between PV installers can reduce  
1142 the cost of installing solar PV. Energy Policy 144, 111600.  
1143 <https://doi.org/10.1016/j.enpol.2020.111600>
- 1144 Ng, P.K., Mithraratne, N., Kua, H.W., 2013. Energy analysis of semi-transparent BIPV in Singapore  
1145 buildings. Energy Build. 66, 274–281. <https://doi.org/10.1016/j.enbuild.2013.07.029>

- 1146 Nikolskaia, A.B., Kozlov, S.S., Vildanova, M.F., Shevaleevskiy, O.I., 2019. Power Conversion  
1147 Efficiencies of Perovskite and Dye-Sensitized Solar Cells under Various Solar Radiation  
1148 Intensities. *Semiconductors* 53, 540–544. <https://doi.org/10.1134/S1063782619040213>
- 1149 Nundy, S., Ghosh, A., 2020. Thermal and visual comfort analysis of adaptive vacuum integrated  
1150 switchable suspended particle device window for temperate climate. *Renew. Energy* 156, 1361–  
1151 1372. <https://doi.org/10.1016/j.renene.2019.12.004>
- 1152 Nundy, S., Ghosh, A., Mallick, T.K., 2020. Hydrophilic and Superhydrophilic Self-Cleaning Coatings  
1153 by Morphologically Varying ZnO Microstructures for Photovoltaic and Glazing Applications.  
1154 *ACS Omega* 5, 1033–1039. <https://doi.org/10.1021/acsomega.9b02758>
- 1155 Nundy, S., Ghosh, A., Tahir, A., Mallick, T.K., 2021a. Role of Hafnium Doping on Wetting  
1156 Transition Tuning the Wettability Properties of ZnO and Doped Thin Films : Self-Cleaning  
1157 Coating for Solar Application. *ACS Appl. Mater. Interfaces* 13, 25540–25552.  
1158 <https://doi.org/10.1021/acscami.1c04973>
- 1159 Nundy, S., Mesloub, A., Alsolami, B.M., Ghosh, A., 2021b. Electrically actuated visible and near-  
1160 infrared regulating switchable smart window for energy positive building : A review. *J. Clean.*  
1161 *Prod.* 301, 126854. <https://doi.org/10.1016/j.jclepro.2021.126854>
- 1162 Ogbomo, O.O., Amalu, E.H., Ekere, N.N., Olagbegi, P.O., 2017. A review of photovoltaic module  
1163 technologies for increased performance in tropical climate. *Renew. Sustain. Energy Rev.* 75,  
1164 1225–1238. <https://doi.org/10.1016/j.rser.2016.11.109>
- 1165 Olivieri, L., Caamaño-Martin, E., Olivieri, F., Neila, J., 2014. Integral energy performance  
1166 characterization of semi-transparent photovoltaic elements for building integration under real  
1167 operation conditions. *Energy Build.* 68, 280–291. <https://doi.org/10.1016/j.enbuild.2013.09.035>
- 1168 Owens, C., Ferguson, G.M., Hermenau, M., Voroshazi, E., Galagan, Y., Zimmermann, B., Rösch, R.,  
1169 Angmo, D., 2016. Comparative Indoor and Outdoor Degradation of Organic Photovoltaic Cells  
1170 via Inter-laboratory Collaboration. *Polymers (Basel)*. 1–8.  
1171 <https://doi.org/10.3390/polym8010001>
- 1172 Parisi, M.L., Maranghi, S., Basosi, R., 2014. The evolution of the dye sensitized solar cells from  
1173 Grätzel prototype to up-scaled solar applications: A life cycle assessment approach. *Renew.*  
1174 *Sustain. Energy Rev.* 39, 124–138. <https://doi.org/10.1016/j.rser.2014.07.079>
- 1175 Parisi, M.L., Sinicropi, A., Basosi, R., 2011. Life cycle assessment of gratzel-type cell production for  
1176 non conventional photovoltaics from novel organic dyes. *Int. J. Heat Technol.* 29, 161–169.
- 1177 Park, K.E., Kang, G.H., Kim, H.I., Yu, G.J., Kim, J.T., 2010. Analysis of thermal and electrical  
1178 performance of semi-transparent photovoltaic (PV) module. *Energy* 35, 2681–2687.  
1179 <https://doi.org/10.1016/j.energy.2009.07.019>
- 1180 Patel, M.T., Vijayan, R.A., Asadpour, R., Varadharajaperumal, M., Khan, M.R., Alam, M.A., 2020.  
1181 Temperature-dependent energy gain of bifacial PV farms : A global perspective. *Appl. Energy*  
1182 276, 115405. <https://doi.org/10.1016/j.apenergy.2020.115405>
- 1183 Peng, J., Curcija, D.C., Lu, L., Selkowitz, S.E., Yang, H., Zhang, W., 2016. Numerical investigation  
1184 of the energy saving potential of a semi-transparent photovoltaic double-skin facade in a cool-  
1185 summer Mediterranean climate. *Appl. Energy* 165, 345–356.  
1186 <https://doi.org/10.1016/j.apenergy.2015.12.074>
- 1187 Peng, J., Lu, L., Yang, H., 2013. Review on life cycle assessment of energy payback and greenhouse  
1188 gas emission of solar photovoltaic systems. *Renew. Sustain. Energy Rev.* 19, 255–274.  
1189 <https://doi.org/10.1016/j.rser.2012.11.035>
- 1190 Qiu, C., Yang, H., Zhang, W., 2019. Investigation on the energy performance of a novel BIPV system  
1191 integrated with vacuum glazing. *Build. Simul.* 12, 29–39.



- 1192 <https://doi.org/https://doi.org/10.1007/s12273-018-0464-6>
- 1193 Quek, G., Wienold, J., Khanie, M.S., Erell, E., Kaftan, E., Tzempelikos, A., Konstantzos, I.,  
1194 Christoffersen, J., Kuhn, T., Andersen, M., 2021. Comparing performance of discomfort glare  
1195 metrics in high and low adaptation levels. *Build. Environ.* 206, 108335.  
1196 <https://doi.org/10.1016/j.buildenv.2021.108335>
- 1197 Research, B., 2018. Perovskite Solar Cells: Materials, Fabrication, and Global Markets.  
1198 [https://doi.org/https://www.bccresearch.com/market-research/energy-and-resources/perovskite-](https://doi.org/https://www.bccresearch.com/market-research/energy-and-resources/perovskite-solar-cells-materials-fabrication-and-global-markets-report.html)  
1199 [solar-cells-materials-fabrication-and-global-markets-report.html](https://doi.org/https://www.bccresearch.com/market-research/energy-and-resources/perovskite-solar-cells-materials-fabrication-and-global-markets-report.html)
- 1200 Rezaei, S.D., Shannigrabi, S., Ramakrishna, S., 2017. A review of conventional, advanced, and smart  
1201 glazing technologies and materials for improving indoor environment. *Sol. Energy Mater. Sol.*  
1202 *Cells* 159, 26–51. <https://doi.org/10.1016/j.solmat.2016.08.026>
- 1203 Richhariya, G., Kumar, A., Tekasakul, P., Gupta, B., 2017. Natural dyes for dye sensitized solar cell:  
1204 A review. *Renew. Sustain. Energy Rev.* 69, 705–718. <https://doi.org/10.1016/j.rser.2016.11.198>
- 1205 Riverola, A., Mellor, A., Alonso Alvarez, D., Ferre Llin, L., Guarracino, I., Markides, C.N., Paul,  
1206 D.J., Chemisana, D., Ekins-Daukes, N., 2018. Mid-infrared emissivity of crystalline silicon solar  
1207 cells. *Sol. Energy Mater. Sol. Cells* 174, 607–615. <https://doi.org/10.1016/j.solmat.2017.10.002>
- 1208 Roy, A., Ghosh, A., Bhandari, S., Selvaraj, P., Sundaram, S., Mallick, T.K., 2019. Color Comfort  
1209 Evaluation of Dye-Sensitized Solar Cell (DSSC) Based Building-Integrated Photovoltaic (BIPV)  
1210 Glazing after 2 Years of Ambient Exposure. *J. Phys. Chem. C* 123, 23834–23837.  
1211 <https://doi.org/10.1021/acs.jpcc.9b05591>
- 1212 Roy, A., Ullah, H., Ghosh, A., Baig, H., Sundaram, S., Tahir, A.A., Mallick, T.K., 2021.  
1213 Understanding the Semi-Switchable Thermochromic Behavior of Mixed Halide Hybrid  
1214 Perovskite Nanorods. *J. Phys. Chem. C* 125, 18058–18070.  
1215 <https://doi.org/10.1021/acs.jpcc.1c05487>
- 1216 Roy, P., Kumar Sinha, N., Tiwari, S., Khare, A., 2020. A review on perovskite solar cells: Evolution  
1217 of architecture, fabrication techniques, commercialization issues and status. *Sol. Energy* 198,  
1218 665–688. <https://doi.org/10.1016/j.solener.2020.01.080>
- 1219 Russell, T.C.R., Saive, R., Bowden, S.G., Atwater, H.A., 2017. The Influence of Spectral Albedo on  
1220 Bifacial Solar Cells : A Theoretical and Experimental Study. *Ieee J. Photovoltaics* 7, 1611–1618.
- 1221 Santbergen, R., van Zolingen, R.J.C., 2008. The absorption factor of crystalline silicon PV cells: A  
1222 numerical and experimental study. *Sol. Energy Mater. Sol. Cells* 92, 432–444.  
1223 <https://doi.org/10.1016/j.solmat.2007.10.005>
- 1224 Sato, R., Chiba, Y., Chikamatsu, M., Yoshida, Y., Taima, T., Kasu, M., Masuda, A., 2019.  
1225 Investigation of the power generation of organic photovoltaic modules connected to the power  
1226 grid for more than three years. *Jpn. J. Appl. Phys.* 58, 052001. [https://doi.org/10.7567/1347-](https://doi.org/10.7567/1347-4065/ab0742)  
1227 [4065/ab0742](https://doi.org/10.7567/1347-4065/ab0742)
- 1228 Sellami, N., Mallick, T.K., McNeil, D.A., 2012. Optical characterisation of 3-D static solar  
1229 concentrator. *Energy Convers. Manag.* 64, 579–586.  
1230 <https://doi.org/10.1016/j.enconman.2012.05.028>
- 1231 Selvaraj, P., Ghosh, A., Mallick, T.K., Sundaram, S., 2019. Investigation of semi-transparent dye-  
1232 sensitized solar cells for fenestration integration. *Renew. Energy* 141, 516–525.  
1233 <https://doi.org/10.1016/j.renene.2019.03.146>
- 1234 Singh, D., Chaudhary, R., Karthick, A., 2021. Review on the progress of building-applied/integrated  
1235 photovoltaic system, *Environmental Science and Pollution Research*. *Environmental Science*  
1236 *and Pollution Research*. <https://doi.org/10.1007/s11356-021-15349-5>

- 1237 Skandalos, N., Karamanis, D., 2015. PV glazing technologies. *Renew. Sustain. Energy Rev.* 49, 306–  
1238 322. <https://doi.org/10.1016/j.rser.2015.04.145>
- 1239 Skoplaki, E., Palyvos, J.A., 2009a. On the temperature dependence of photovoltaic module electrical  
1240 performance: A review of efficiency/power correlations. *Sol. Energy* 83, 614–624.  
1241 <https://doi.org/10.1016/j.solener.2008.10.008>
- 1242 Skoplaki, E., Palyvos, J.A., 2009b. Operating temperature of photovoltaic modules: A survey of  
1243 pertinent correlations. *Renew. Energy* 34, 23–29. <https://doi.org/10.1016/j.renene.2008.04.009>
- 1244 Sorgato, M.J., Schneider, K., Rütger, R., 2018. Technical and economic evaluation of thin-film CdTe  
1245 building-integrated photovoltaics (BIPV) replacing façade and rooftop materials in office  
1246 buildings in a warm and sunny climate. *Renew. Energy* 118, 84–98.  
1247 <https://doi.org/10.1016/j.renene.2017.10.091>
- 1248 Soria, B., Gerritsen, E., Lefillastre, P., Broquin, J., 2016. A study of the annual performance of  
1249 bifacial photovoltaic modules in the case of vertical facade integration. *Energy Sci. Eng.* 4, 52–  
1250 68. <https://doi.org/10.1002/ese3.103>
- 1251 Stuckelberger, M., Biron, R., Wyrsh, N., Haug, F.-J., Ballif, C., 2017. Review: Progress in solar cells  
1252 from hydrogenated amorphous silicon. *Renew. Sustain. Energy Rev.* 76, 1–27.  
1253 <https://doi.org/10.1016/j.rser.2016.11.190>
- 1254 Sun, Y., Liu, D., Flor, J.F., Shank, K., Baig, H., Wilson, R., Liu, H., Sundaram, S., Mallick, T.K., Wu,  
1255 Y., 2020. Analysis of the daylight performance of window integrated photovoltaics systems.  
1256 *Renew. Energy* 145, 153–163. <https://doi.org/10.1016/j.renene.2019.05.061>
- 1257 Systems, F.I. for S.E., 2021. Photovoltaics Report.  
1258 [https://doi.org/https://www.ise.fraunhofer.de/content/dam/ise/de/documents/publications/studies/  
1259 Photovoltaics-Report.pdf](https://doi.org/https://www.ise.fraunhofer.de/content/dam/ise/de/documents/publications/studies/Photovoltaics-Report.pdf)
- 1260 Tait, D.B., 2006. for High-Mass Glazing Blocks. *ASHRAE Trans.* 112, 142–150.
- 1261 Tällberg, R., Jelle, B.P., Loonen, R., Gao, T., Hamdy, M., 2019. Comparison of the energy saving  
1262 potential of adaptive and controllable smart windows: A state-of-the-art review and simulation  
1263 studies of thermochromic, photochromic and electrochromic technologies. *Sol. Energy Mater.*  
1264 *Sol. Cells* 200, 109828. <https://doi.org/10.1016/j.solmat.2019.02.041>
- 1265 Tasgas, I., 2021. Exceeding all expectations. *PV Mag.* [https://doi.org/https://www.pv-  
1266 magazine.com/magazine-archive/exceeding-all-expectations/](https://doi.org/https://www.pv-magazine.com/magazine-archive/exceeding-all-expectations/)
- 1267 Tian, H., Yu, X., Zhang, J., Duan, W., Tian, F., Yu, T., 2012. The influence of environmental factors  
1268 on DSSCs for BIPV. *Int. J. Electrochem. Sci.* 7, 4686–4691.
- 1269 Tong, G., Son, D., Ono, L.K., Liu, Y., Hu, Y., Zhang, H., Jamshaid, A., Qiu, L., Liu, Z., Qi, Y., 2021.  
1270 Scalable Fabrication of > 90 cm<sup>2</sup> Perovskite Solar Modules with > 1000 h Operational Stability  
1271 Based on the Intermediate Phase Strategy 2003712, 1–11.  
1272 <https://doi.org/10.1002/aenm.202003712>
- 1273 Virtuani, A., Pavanello, D., Friesen, G., 2010. OVERVIEW OF TEMPERATURE COEFFICIENTS  
1274 OF DIFFERENT THIN FILM PHOTOVOLTAIC TECHNOLOGIES, in: 25th European  
1275 Photovoltaic Solar Energy Conference and Exhibition/5th World Conference on Photovoltaic  
1276 Energy Conversion. Valencia, pp. 6–10.
- 1277 Wang, C., Yu, S., Guo, X., Chen, J., Wang, C., Yu, S., Guo, X., Kearney, T., Guo, P., Chang, R.,  
1278 2020. Article Maximizing Solar Energy Utilization through Multicriteria Pareto Optimization of  
1279 Energy Harvesting and Regulating Smart Windows Maximizing Solar Energy Utilization  
1280 through Multicriteria Pareto Optimization of Energy Harvesting and Regulating Smart  
1281 Windows. *Cell Reports Phys. Sci.* 1, 100108. <https://doi.org/10.1016/j.xcrp.2020.100108>

- 1282 Wheeler, L.M., Moore, D.T., Tenent, R.C., Blackburn, J.L., Ihly, R., Stanton, N.J., Miller, E.M.,  
 1283 Neale, N.R., 2017. Switchable photovoltaic windows enabled by reversible photothermal  
 1284 complex dissociation from methylammonium lead iodide. *Nat. Commun.*  
 1285 <https://doi.org/10.1038/s41467-017-01842-4>
- 1286 Wienold, J., Christoffersen, J., 2006. Evaluation methods and development of a new glare prediction  
 1287 model for daylight environments with the use of CCD cameras. *Energy Build.* 38, 743–757.  
 1288 <https://doi.org/10.1016/j.enbuild.2006.03.017>
- 1289 Wienold, J., Iwata, T., Sarey Khanie, M., Erell, E., Kaftan, E., Rodriguez, R.G., Yamin Garretton,  
 1290 J.A., Tzempelikos, T., Konstantzos, I., Christoffersen, J., Kuhn, T.E., Pierson, C., Andersen, M.,  
 1291 2019. Cross-validation and robustness of daylight glare metrics, *Lighting Research and*  
 1292 *Technology.* <https://doi.org/10.1177/1477153519826003>
- 1293 Wilson, C.F., Simko, T.M., Collins, R.E., 1998. Heat conduction through the support pillars in  
 1294 vacuum glazing. *Sol. Energy* 63, 393–406. [https://doi.org/10.1016/S0038-092X\(98\)00079-6](https://doi.org/10.1016/S0038-092X(98)00079-6)
- 1295 Yan, F., Noble, J., Peltola, J., Wicks, S., Balasubramanian, S., 2013. Semitransparent OPV Modules  
 1296 Pass Environmental Chamber Test Requirements. *Sol. Energy Mater. Sol. Cells* 114, 214–218.  
 1297 <https://doi.org/10.1016/j.solmat.2012.09.031>
- 1298 Yoon, S., Tak, S., Kim, J., Jun, Y., Kang, K., Park, J., 2011. Application of transparent dye-sensitized  
 1299 solar cells to building integrated photovoltaic systems. *Build. Environ.* 46, 1899–1904.  
 1300 <https://doi.org/10.1016/j.buildenv.2011.03.010>
- 1301 Zhang, T., Wang, M., Yang, H., 2018. A review of the energy performance and life-cycle assessment  
 1302 of building-integrated photovoltaic (BIPV) systems. *Energies* 11.  
 1303 <https://doi.org/10.3390/en11113157>
- 1304 Zhang, W., Lu, L., Chen, X., 2017. Performance evaluation of vacuum photovoltaic insulated glass  
 1305 unit. *Energy Procedia* 105, 322–326. <https://doi.org/10.1016/j.egypro.2017.03.321>
- 1306 Zhang, W., Lu, L., Peng, J., Song, A., 2016. Comparison of the overall energy performance of semi-  
 1307 transparent photovoltaic windows and common energy-efficient windows in Hong Kong.  
 1308 *Energy Build.* 128, 511–518. <https://doi.org/10.1016/j.enbuild.2016.07.016>
- 1309 Zhang, Y., Tso, C.Y., Iñigo, J.S., Liu, S., Miyazaki, H., Chao, C.Y.H., Yu, K.M., 2019. Perovskite  
 1310 thermochromic smart window: Advanced optical properties and low transition temperature.  
 1311 *Appl. Energy* 254. <https://doi.org/10.1016/j.apenergy.2019.113690>
- 1312 Zhao, J., Luo, S., Zhang, X., Xu, W., 2013. Preparation of a transparent supporting spacer array for  
 1313 vacuum glazing. *Vacuum* 93, 60–64. <https://doi.org/10.1016/j.vacuum.2013.01.002>
- 1314 Zhao, J.F., Eames, P.C., Hyde, T.J., Fang, Y., Wang, J., 2007. A modified pump-out technique used  
 1315 for fabrication of low temperature metal sealed vacuum glazing. *Sol. Energy* 81, 1072–1077.  
 1316 <https://doi.org/10.1016/j.solener.2007.03.006>
- 1317 Zhou, Z., Carbajales-Dale, M., 2018. Assessing the photovoltaic technology landscape: Efficiency  
 1318 and energy return on investment (EROI). *Energy Environ. Sci.* 11, 603–608.  
 1319 <https://doi.org/10.1039/c7ee01806a>
- 1320 Zhu, L., Raman, A., Wang, K.X., Anoma, M.A., Fan, S., 2014. Radiative cooling of solar cells.  
 1321 *Optica* 1, 32. <https://doi.org/10.1364/optica.1.000032>
- 1322 Zidane, T.E.K., Adzman, M.R. Bin, Tajuddin, M.F.N., Mat Zali, S., Durusu, A., 2019. Optimal  
 1323 configuration of photovoltaic power plant using grey wolf optimizer: A comparative analysis  
 1324 considering CdTe and c-Si PV modules. *Sol. Energy* 188, 247–257.  
 1325 <https://doi.org/10.1016/j.solener.2019.06.002>
- 1326